Precambrian Research 294 (2017) 15–32

Contents lists available at ScienceDirect

Precambrian Research

journal homepage: www.elsevier.com/locate/precamres

The origin of Patagonia revealed by Re-Os systematics of mantle xenoliths

Manuel Enrique Schilling [a,*], Richard Walter Carlson [b], Andrés Tassara [c], Rommulo Vieira Conceição [d], Gustavo Walter Bertotto [e], Manuel Vásquez [f], Daniel Muñoz [f], Tiago Jalowitzki [d], Fernanda Gervasoni [g], Diego Morata [f,h]

[a] Instituto de Ciencias de la Tierra, Facultad de Ciencias, Universidad Austral de Chile, Campus Isla Teja, Valdivia 5090000, Región de Los Ríos, Chile
[b] Department of Terrestrial Magnetism, Carnegie Institution for Science, 5241 Broad Branch Road, NW Washington, DC 20015-1305, USA
[c] Departamento de Ciencias de la Tierra, Universidad de Concepción, Casilla 160-C, Barrio Universitario, Concepción, Chile
[d] Instituto de Geociências, Universidade Federal do Rio Grande do Sul, Av. Bento Gonçalves 9500, prédio 43129, CEP 91501-970, Porto Alegre, Brazil
[e] CONICET y Facultad de Ciencias Exactas y Naturales, Universidad Nacional de la Pampa, Av. Uruguay 151, Santa Rosa, La Pampa, Argentina
[f] Departamento de Geología, Facultad de Ciencias Físicas y Matemáticas, Universidad de Chile, Plaza Ercilla 803, Santiago, Chile
[g] Institut für Mineralogie, Westfählische–Wilhelms–Universität Münster, Corrensstraße 24, D-48149 Münster, Germany
[h] Centro de Excelencia en Geotermia de los Andes (CEGA), Facultad de Ciencias Físicas y Matemáticas, Universidad de Chile, Plaza Ercilla 803, Santiago, Chile

ARTICLE INFO

Article history:
Received 15 October 2016
Revised 1 March 2017
Accepted 7 March 2017
Available online 11 March 2017

Keywords:
Patagonia
Mantle xenoliths
Os isotopes
Proterozoic
Rodinia

ABSTRACT

We present mineral chemistry and whole rock major, trace, and platinum group element (PGE) concentrations, and Re-Os isotope data for eighteen mantle xenoliths carried to the surface of southern Patagonia (45°–52°S) by Paleocene to Pleistocene alkaline basalts in seven localities scattered widely across southern South America. The new data along with those previously published show that peridotites derived from the lithospheric mantle of the Deseado Massif (DM), southern Patagonia, have compositions indicative of higher degrees of partial melt extraction compared to those from surrounding regions. Re-depletion model ages (T_{RD}) of mantle xenoliths from the DM (n = 20) range from 0.5 to 2.1 Ga, with an average of 1.5 Ga. In contrast, samples from the surrounding areas (n = 39) have a wider range of Re-depletion ages from 0.0 to 2.5 Ga, with an average of 1.0 Ga. Similar geochemical characteristics are recognized between the lithospheric mantle section of the DM and that beneath East Griqualand (~1.1 Ga), south-eastern Africa, which is related to the Proterozoic Namaqua-Natal Province. The Re-Os systematics of the mantle xenoliths are indicative of Meso to Paleoproterozoic ages for partial melting and stabilization processes of the lithospheric mantle of southern Patagonia, which are considerably older than the crystallization ages obtained for the scarce basement rocks of Patagonia (<0.6 Ga). In addition, published elastic thickness (T_e) estimates of southern South America show maximum values on the submerged continental region located between the DM and the Malvinas/Falkland Islands, where Grenville-age metamorphic rocks are exposed. These geochemical and geophysical results suggest that southern Patagonia and the Malvinas/Falkland Islands and plateau constitute an integrated and relatively rigid continental block formed mainly during the Meso to Paleoproterozoic as part of the supercontinent Rodinia.

To the north, the formation of the North Patagonian Massif (NPM) seems to be contemporaneous with that of the DM. Nevertheless, its ancient lithospheric mantle and lower crust appear to have been widely eroded and replaced by relatively young convecting mantle, possibly during the Carboniferous collision between the DM and the NPM. The differences between the DM and NPM lithosphere histories apparently controlled the subsequent formation and distribution of Jurassic epithermal Au-Ag deposits.

1. Introduction

The study of mantle xenoliths has revealed significant information about the physical, thermal, compositional, and chronological history of the subcontinental lithospheric mantle (e.g. Pearson

* Corresponding author.
E-mail address: manuel.schilling@uach.cl (M.E. Schilling).

http://dx.doi.org/10.1016/j.precamres.2017.03.008
0301-9268/

et al., 2003). Important differences have been recognized between the lithospheric mantle beneath Archean cratons, and that beneath Proterozoic and Phanerozoic terranes. Higher thermal gradients in the mantle during the Archean resulted in higher degrees of partial melting that led to notably lower concentrations of Al_2O_3 and CaO, lower garnet and clinopyroxene modal percentages, and higher olivine forsterite contents in cratonic mantle residues compared to the lithospheric mantle beneath Proterozoic and Phanerozoic continental regions (e.g. Carlson et al., 2005; Griffin et al., 2003, 2009, 1999; Pearson et al., 2003). The high degrees of melt extraction generated cold, strong and buoyant continental mantle that contributed to the formation and stabilization of the continental lithosphere over Earth history (e.g. Carlson et al., 2005).

The Re-Os isotopic system ($^{187}Re \rightarrow {}^{187}Os + \beta^-$; $\lambda = 1.666 \times 10^{-11}\ yr^{-1}$; Smoliar et al., 1996) has been widely used for dating mantle melt extraction events, and consequently, the time of lithospheric mantle formation. The application of the Re-Os system to this problem has been extensively discussed (Carlson, 2005; Rudnick and Walker, 2009; Shirey and Walker, 1998; Walker et al., 1989). Several studies have shown that there is a general correspondence between the age of the crust and the age of its underlying mantle (Aulbach et al., 2004; Carlson and Moore, 2004; Griffin et al., 2004; Hanghøj et al., 2001; Irvine et al., 2003; Pearson et al., 2002). Regarding the platinum group element (PGE: Os, Ir, Ru, Pt, Pd) abundances, cratonic mantle samples are generally characterized by highly depleted PPGE (Pd and Pt) abundances, compared to the IPGE (Os, Ir, and Ru), as a consequence of the more compatible behavior of the IPGE during mantle melting (e.g. Pearson et al., 2004 and references therein). Moreover, different geophysical approaches based on heat flow, gravity and seismic data, also show significantly thicker, colder and more rigid continental lithosphere beneath ancient continents compared to younger crustal terrains (e.g. Ritsema et al., 2004; Tassara et al., 2007).

In this work we report new mineral chemistry and whole rock major, trace, and platinum group element (PGE) abundances, as well as Re-Os isotope data for 18 mantle xenoliths from southern Patagonia (Fig. 1) with the goal of defining the age distribution of distinct terranes so that the tectonic history of continental assembly in this area can be better understood. The new data support and complement previous results (Mundl et al., 2016, 2015; Schilling et al., 2008; Stern et al., 1999). Furthermore, we discuss the apparent connection between the physical and chemical heterogeneities of the Patagonian lithosphere and the occurrence of epithermal Au–Ag deposits related to the Jurassic volcanic magmatism produced during the fragmentation of Gondwana (Moreira and Fernández, 2015; Schalamuk et al., 1997).

2. Geological setting

Patagonia conventionally has been considered as the continental region of southern South America located south of the Colorado River. Patagonia displays significant differences to the rest of the continent in terms of topography, environment, flora, fauna and paleontological record. Based on geophysical data, the physiographic boundary of Patagonia has been moved south to the line of the Huincul fault (Ramos et al., 2004). This line is coincident with an E-W trending magnetic and gravity anomaly located immediately to the south of 39°S (Fig. 1), that marks a break in the distinct N-S structures of the Chilenia, Cuyania and Pampia terranes, as well as those of the Río de la Plata craton, to the north (Chernicoff and Zappettini, 2004; Kostadinoff et al., 2005; Ramos et al., 2004). The origin of Patagonia as an independent continental block has been the subject of a long debate (Frutos and Tobar, 1975; Keidel, 1925; Pankhurst et al., 2006; Ramos, 2008, 2002,

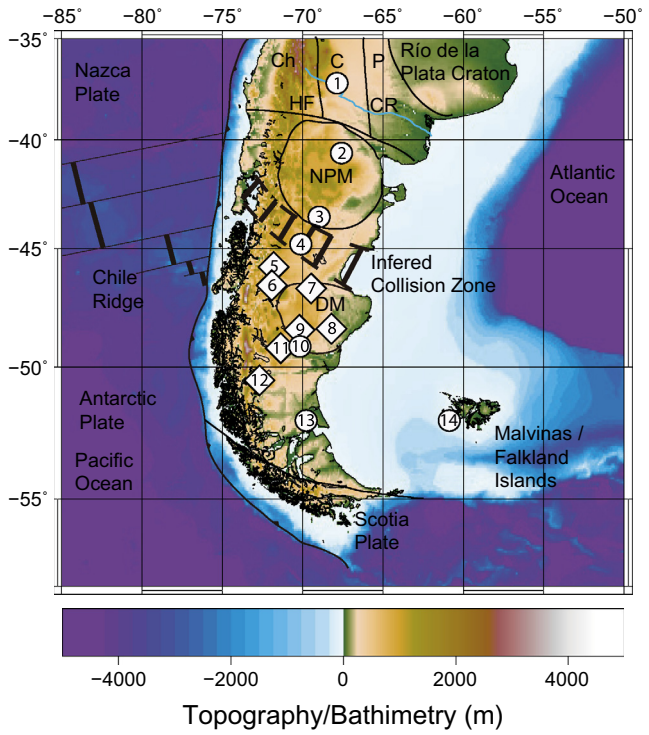

Fig. 1. Location of mantle xenoliths and other relevant localities on topography/bathymetry map of southern South America. Abbreviations: C: Cuyania terrane; Ch: Chilenia terrane; CR: Colorado River; DM: Deseado Massif; HF: Huincul Fault; NPM: North Patagonian Massif; P: Pampia terrane. The numbers correspond to the following localities (diamonds indicate samples of the present study): 1, Agua Poca; 2, Prahuaniyeu; 3, Paso de Indios; 4, Cerro de los Chenques; 5, Coyhaique; 6, Chile Chico; 7 Cerro Clark; 8, Auvernia; 9, Gobernador Gregores (Estancia Lote 17); 10, Cerro Redondo; 11, Tres Lagos; 12, Cerro del Fraile; 13, Pali Aike, and 14, Cape Meredith (Cabo Belgrano).

1984). However, the understanding of the early history of Patagonia has been limited by very small and scarce outcrops of continental basement rocks, with most of the older basement covered by extensive amounts of volcanic rocks and sediments.

The Precambrian geological record of Patagonia is mainly recorded by Mesoproterozoic Nd model ages (1.0–1.6 Ga) calculated for diverse and widely distributed Phanerozoic igneous rocks (Martínez Dopico et al., 2011; Pankhurst et al., 2006, 2003; Pankhurst and Rapela, 1995), and the provenance ages for detrital zircons contained in metasedimentary rocks. Populations of detrital zircon grains have typically Gondwana-age components ranging mainly from 460 to 750 Ma and 1000 to 1200 Ma, as well as a small component of older ages, including some at 1750–2000, 2000–2200 and 2550–2700 Ma (Chernicoff et al., 2013; Hervé et al., 2013, 2003; Moreira et al., 2013; Pankhurst et al., 2006, 2003). In contrast, to the north of Patagonia, Grenville-age continental crust (~1.0–1.2 Ga) has been recognized on the Pampia (e.g. Casquet et al., 2006) and Cuyania (e.g. Kay et al., 1996; Sato et al., 2000) continental terranes. These two terranes collided with the western proto-margin of Gondwana, represented by the 2.0–2.2 Ga Río de la Plata craton (Rapela et al., 2007), during the Early Cambrian (Pampean orogenic cycle) and Middle Ordovician (Famatinian orogenic cycle), respectively (e.g. Vujovich et al., 2004). Towards the east and southeast of the Deseado Massif (DM), Grenville-age metamorphic rocks are found at Cape Meredith (or Cabo Belgrano) in the Malvinas/Falkland Islands (Cingolani and Varela, 1976; Jacobs et al., 1999; Rex and Tanner, 1982), which are located on the extension of the continental shelf of southern South America. These Proterozoic ages have supported the idea that the Malvinas/Falkland Islands previously formed an easterly

extension of the Natal sector of the Proterozoic Namaqua-Natal province of southern South Africa, and consequently have been considered as a microplate related to the Grenville-age (1.0–1.2 Ga) supercontinent Rodinia (e.g. Thomas et al., 2000; Wareham et al., 1998). However, the location and tectonic character of the margin between the hypothetical Malvinas/Falkland Islands microplate and the Deseado terrane have not yet been documented (Pankhurst et al., 2006).

Concerning the Phanerozoic geologic evolution of Patagonia, the study of the basement rocks of the Sierra de la Ventana belt performed by Rapela et al. (2003) revealed a Cambrian rifting event that separated the 600 Ma Neoproterozoic crust of the North Patagonian Massif (NPM) from the rest of the continent, producing crustal melting and the deposition of lower to middle Paleozoic marine sediments in gently subsiding basins. According to these authors, the Cambrian continental passive margin that developed at the Sierra de la Ventana belt also extended into the Cape fold belt in southern Africa, the Falkland/Malvinas Islands and the Ellsworth Mountains in Antarctica. In most tectonic models, southern Patagonia, corresponding to the DM, has been described as an independent continental block that collided and amalgamated to the NPM during western Gondwana assembly, but there is no consensus yet about its origin and the timing and plate configurations related to its accretion. Diverse tectonic models describing the tectonic assembly of these terranes have been proposed (Pankhurst et al., 2006, 2003; Ramos, 2008, 2002, 1984; Rapela et al., 2003).

During the Permian and Triassic, northern Patagonia experienced voluminous and widespread silicic plutonism and volcanism, referred to as the Choiyoi province (Pankhurst et al., 2006). At that time, southern Patagonia was affected by tectonic extension and rifting that preceded late disaggregation of Gondwana (e.g. Homovc and Constantini, 2001). The subsequent continental fragmentation was related to middle-upper Jurassic crustal stretching. The stretching drove partial melting that produced widespread bimodal volcanic and volcano-sedimentary rocks, known as the Chon Aike province (Pankhurst et al., 1998). This Jurassic large igneous province covers a wide area of southern South America extending to the Antarctic Peninsula. In the DM, these volcanic rocks are related to the formation of numerous and important Au-Ag epithermal deposits (Echavarría et al., 2005; Fernández et al., 2008; Giacosa et al., 2010; Moreira and Fernández, 2015; Schalamuk et al., 1997). Pankhurst and Rapela (1995) obtained neodymium model ages of 1.1–1.6 Ga for Jurassic andesitic rocks from Patagonia and suggested an origin by anatexis of a Grenville-age mafic lower crust. The Mesozoic breakup of Gondwana has been better constrained by the refined and integrated plate tectonic model of König and Jokat (2006), where the large dextral strike-slip movement (more than 1000 km) between southern South America, represented by the Malvinas/Falkland Plateau, and southern South Africa was controlled by the Agulhas Falkland Fracture Zone (AFFZ). Since then, the geological evolution of the southwestern margin of South America was controlled by a relatively continuous subduction process related to the Andean orogenesis and the recycling of various oceanic plates beneath the continent (Mpodozis and Ramos, 1989).

During the Cenozoic, extensive basaltic flows derived from an asthenospheric mantle source erupted over large areas of the southern Andean and Patagonian back-arc region (Gorring et al., 1997; Gorring and Kay, 2001; Ramos and Kay, 1992; Stern et al., 1990). Many of these basalts contain mantle xenoliths that have been studied with the aim of characterizing the subcontinental lithospheric mantle of this region (Bjerg et al., 2005; Conceição et al., 2005; Gorring and Kay, 2000; Jalowitzki et al., 2016; Laurora et al., 2001; Mundl et al., 2016, 2015; Ntaflos et al., 2007; Rivalenti et al., 2007, 2004, Schilling et al., 2005, 2008; Stern et al., 1999, among many others). Measurements of $^{187}Os/^{188}Os$ ratios on Patagonian mantle xenoliths have demonstrated the existence of heterogeneous lithospheric mantle domains formed at different times (Mundl et al., 2016, 2015; Schilling et al., 2008; Stern et al., 1999). Samples from the NPM yield Os isotopic compositions similar to the present suboceanic mantle, suggesting a relatively recent lithospheric mantle formation from the convecting mantle. The one exception in the NPM is the Prahuaniyeu xenolith locality that also included Mesoproterozoic Os model ages (Mundl et al., 2015; Schilling et al., 2008) resembling those of peridotites from Agua Poca derived from the lithospheric mantle of the Grenville-age Cuyania continental block (Schilling et al., 2008). Proterozoic T_{RD} model ages (1.3–1.8 Ga) have been found for peridotites from the southwestern edge of the DM (Gobernador Gregores, Cerro Redondo and Tres Lagos), which are considerably older than the crystallization ages known for the oldest basement continental rocks (~0.6 Ga) suggesting the existence of a hidden ancient lithosphere, probably related to the Namaqua-Natal orogenic belt of South Africa (Mundl et al., 2015; Schilling et al., 2008). Remarkably, the oldest T_{RD} ages (up to 2.5 Ga) were determined for Pali Aike peridotites by Mundl et al. (2015). These authors suggested a potential common origin with the Paleoproterozoic continental lithosphere of the Shackleton Range located at the northwestern edge of the East Antarctic craton, where similar ages have been reported.

3. Samples

The mantle xenoliths for this study (Supplementary Fig. 1) were selected from a large set of samples collected at different localities during two expeditions to Patagonia in Argentina and Chile with the aim to complement published Os isotopic data available on the area of the DM (Fig. 1, Supplementary Table 1). Specifically, anhydrous spinel-peridotites were chosen from five localities previously studied (Tres Lagos, Gobernador Gregores, Cerro del Fraile, Cerro Clark and Chile Chico), and from two new localities (Auvernia volcano and Coyhaique). The oldest eruption age is the Coyhaique locality; an alkaline basaltic lava flow dated at 58.6 ± 2 Ma using the whole rock K-Ar method (De la Cruz et al., 2003). The Chile Chico mantle xenoliths are found in an alkali basalt volcanic neck that was dated using the same method at 40.7 ± 1.4 Ma (Espinoza, 2003). Mantle xenoliths from Cerro Clark are found in a volcanic neck composed of porphyritic basanite of possible Miocene age (11–12 Ma), based on the work of Gorring et al. (1997) that presented whole rock $^{40}Ar/^{39}Ar$ ages for proximate lavas. In the same way, an age between 4 and 7 Ma is estimated for the spatter cone containing the mantle xenoliths of Tres Lagos. Many of these xenoliths are included in volcanic bombs. Gobernador Gregores mantle samples are associated with basanitic surge deposits in a post-plateau sequence of Pliocene age (~3.5 Ma) as defined by Gorring et al. (1997) and Gorring and Kay (2000). An age of 1–2 Ma was determined for the Cerro del Fraile alkali basalt using $^{40}Ar/^{39}Ar$ step-heating and unspiked K-Ar methods (Singer et al., 2013). This locality is the closest to the Chile trench (~280 km) followed by Coyhaique and Chile Chico (~300 km). Finally, Auvernia volcano erupted less than 1 Ma ago (Panza, 1994), and is the eastern most occurrence of mantle xenoliths on the DM, located ~580 km from the Chile trench.

To investigate the partial melting events that occurred in the subcontinental lithospheric mantle at regional scales, peridotites from the DM and surrounding regions were chosen based on their low Al_2O_3 contents that define them as residues of higher degrees of melt extraction. Re-depletion model ages are most accurate for residues of extensive partial melt removal as the model age calculation assumes that all Re was extracted with the partial melt, which is true only at high degrees of melting. Anhydrous peri-

dotites that have similar Al_2O_3 and CaO concentrations were selected in order to avoid mantle rocks with clear evidence of subsequent metasomatic processes, particularly the introduction of Ca via carbonatite metasomatism. The mantle xenoliths are of variable sizes and shapes. The largest are those found at Tres Lagos, Gobernador Gregores, Cerro Clark and Coyhaique, the largest of which have diameters of more than 20 cm. Samples found at Chile Chico, Cerro del Fraile, and Auvernia volcano are considerably smaller with maximum diameters of 15 cm. The peridotitic xenoliths are relatively fresh, with the exception of samples from Coyhaique that exhibit yellowish to reddish colors, possibly due to post-eruption alteration.

The rock types, textures and modal compositions are summarized in Table 1, together with temperatures of equilibration estimated using the two-pyroxene geothermometer of Brey and Köhler (1990). Modal compositions were estimated by mass balance of whole rock and mineral compositions allowing the classification of our samples as 13 lherzolites and 5 harzburgites. The textures are mainly protogranular, porphyroblastic and transitional between these two types. Only one sample from Gobernador Gregores (PM23-3) exhibits a transitional texture from porphyroblastic to equigranular. Many samples show secondary textures, such as lamellae of exsolution and spongy rims in pyroxenes, and some olivine crystals show kink bands reflecting deformation processes. Lherzolite PM21-1A and harzburgite PM21-6A from Tres Lagos are the only composite xenoliths of the whole set. These two samples contain veins a few centimeters wide of olivine websterite, probably crystallized from percolating metasomatic melts (Pressi, 2008). Fragments selected for chemical analysis of these two samples did not include veins of pyroxenite. Additionally, melt veins related to host basalt infiltration were observed only in small samples (Supplementary Fig. 1, PM20-22; PM26-5; PM27B-1B; PM27B-2; PM27B-12B). In addition to the main mineral phases olivine, orthopyroxene, clinopyroxene and spinel, the studied mantle rocks commonly contain tiny sulfides representing typically less than 1% of the mineral mode (Supplementary Fig. 2). The sulfides have diameters ranging from <20 to 150 μm and occur either interstitially or as rounded inclusions in silicates, preferentially in olivine and orthopyroxene, and sometimes in the form of sulfide trails. Interstitial sulfides are commonly irregularly shaped and can be found between grains of the dominant phases, in melt pockets or around spongy pyroxenes.

4. Analytical techniques

Samples were cut using a rock saw. Fragments of fresh interior materials were used to produce thin sections for petrography and mineral chemistry analysis. Other interior slabs were crushed and ground in an agate mortar to fine powders for whole rock chemical analysis. Rough crushed materials of small samples were carefully inspected under a binocular microscope to remove fragments derived from the host basalt. Mineral major-element compositions of fourteen samples were determined by electron microprobe under accelerating voltages of 15 kV, a beam current from 20 to 30 nA and 10 to 30 s counting time, using natural and synthetic standards for calibration: eight samples were measured at the GEA Institute at the Universidad de Concepción using a JEOL JXA-8600; four samples were analyzed at the Geophysical Laboratory of the Carnegie Institution using a JEOL JXA-8900 SuperProbe; and mineral chemistry of two samples was determined using a CAMECA SX50 electron microprobe at the Paul Sabatier University. Bulk-rock major element compositions of thirteen samples were measured by a PANalytical AXIOS-Advanced X-ray fluorescence (XRF) spectrometer at the laboratory of SERNAGEOMIN. Five duplicates of samples were determined using a ThermoARL Advant'XP+ sequential XRF spectrometer at the GeoAnalytical Lab of the Washington State University. Major element compositions

Table 1
Summary of petrographic characteristics of Patagonian mantle xenoliths including the type and texture of rocks, mineral modes and temperatures of equilibration.

Locality/sample	Type	Texture	Ol	Opx	Cpx	Sp	T (°C)
Coyhaique							
PM25-8	lherz	prot	59.6	27.5	11.0	1.9	1057
PM25-10	lherz	porph	67.3	24.6	6.5	1.6	1040
Chile Chico							
PM26-4	lherz	prot	68.3	18.4	11.4	1.9	–
PM26-5	lherz	prot-porph	64.5	27.1	6.7	1.7	–
Cerro Clark							
PM24-21*	lherz	porph	49.0	33.0	15.0	3.0	–
PM24-41	lherz	prot	62.7	27.7	7.8	1.8	850
Auvernia Volcano							
PM27A-9	lherz	prot	84.8	5.9	8.2	1.1	1021
PM27B-1b	harz	prot	85.4	8.7	4.8	1.1	968
PM27B-2	harz	prot-porph	77.3	18.0	4.3	0.4	1064
PM27B-12b	harz	prot	73.3	20.4	4.9	1.4	–
Gobernador Gregores							
PM23-3	lherz	porph-equi	61.6	25.5	10.2	2.7	1132
PM23-21	lherz	prot-porph	63.5	23.9	10.2	2.4	–
Tres Lagos**							
PM21-1A	lherz	porph	66.3	17.1	14.3	2.3	n.c.
PM21-6A	harz	prot-porph	76.3	18.8	2.4	2.5	n.c.
PM21-9	harz	prot-porph	77.6	18.4	2.6	1.4	n.c.
Cerro del Fraile							
PM20-8	lherz	prot-porph	70.7	19.1	8.6	1.6	–
PM20-20	lherz	prot	55.8	35.6	5.9	2.7	–
PM20-22	lherz	prot	78.2	13.7	5.5	2.6	–

Abbreviations are lherz: lherzolite; harz: harzburgite; prot: protogranular; porph: porphyroclastic; equi: equigranular; Ol: olivine; Opx: orthopyroxene; Cpx: clinopyroxene; and Sp: spinel. Temperatures of equilibration estimated using the geothermometer of Brey and Köhler (1990) at an assumed pressure of 15 kbar. Modal proportions were calculated by chemical balance between mineral and whole rock compositions except for samples (*) and (**) taken from Dantas et al. (2009) and Pressi (2008), respectively. (n.c.), temperatures not calculated; and (–) values discarded for samples showing chemical disequilibrium between clinopyroxene and orthopyroxene according to the Fe-Mg exchange coefficients.

for mantle xenoliths from Coyhaique and Tres Lagos were determined at the Actlabs laboratory by sample fusion and inductively coupled plasma optical emission spectrometry (ICP-OES). Trace element compositions of fourteen samples were determined using the inductively coupled plasma mass spectrometer (ICP-MS) Agilent 7700 at the GeoAnalytical Lab. Long-term precision for the method is typically better than 5% (RSD) for the REEs and 10% for the remaining trace elements.

Re-Os isotopic compositions and platinum group element (PGE) contents were determined at the Department of Terrestrial Magnetism (DTM), Carnegie Institution for Science by the isotope dilution method. One gram of sample powder was digested using 6 ml of reverse aqua regia (2:1 HNO_3-HCl) at high-temperature (~240 °C) in Pyrex Carius tubes over a period of 24–72 h (Shirey and Walker, 1995), together with mixed spikes of ^{185}Re-^{190}Os and ^{191}Ir-^{99}Ru-^{194}Pt-^{105}Pd. Os was separated by solvent extraction employing high-purity CCl_4 and microdistillation in HBr following established techniques (e.g. Reisberg and Meisel, 2002). Rhenium, Ir, Pt and Pd were separated via anion exchange chromatography using AG1X8 resin. Os isotopic compositions were determined by negative thermal ionization mass spectrometry (N-TIMS) using the Thermo-Fisher Triton at DTM. Os was analyzed as OsO_3^- by single-collector peak-hopping in the electron multiplier. Measurements of the DTM J-M Os standard using this procedure during this study gave an average value of $^{187}Os/^{188}Os = 0.17395 \pm 7 (2\sigma)$. This value is within error of the mean of high-precision measurements of this standard using faraday cups of $0.1739255 \pm 10 (2\sigma)$. Total procedural blanks at DTM were less than 2 pg for Re, Os, Ir and Ru, 20 pg for Pd and 30 pg for Pt. Rhenium, Ir, Ru, Pt and Pd concentrations were determined using the Nu Plasma HR multi-collector ICP-MS at DTM.

5. Results

5.1. Mineral chemistry and equilibrium temperature

Mineral composition data for olivine, orthopyroxene, clinopyroxene, and spinel are presented in Supplementary Tables 2, 3, 4 and 5, respectively. The olivine magnesium numbers ($Mg\# = 100 \times Mg/(Mg + Fe_{tot})$ in atomic units), equivalent to forsterite (Fo) contents, vary from 90.0 to 91.7, except for sample PM20-22 from Cerro del Fraile that shows a considerably lower value ($Fo_{88.3}$). NiO and MnO contents range from 0.35 to 0.39 wt % and from 0.11 to 0.17 wt%, respectively, while CaO contents are lower than 0.09%. Orthopyroxene contents of enstatite (En), ferrosilite (Fs) and wollastonite (Wo) vary in the range $En_{89.1\text{-}91.1}$, $Fs_{8.0\text{-}9.7}$, and $Wo_{0.5\text{-}1.8}$, and Mg# range from 90.40 to 92.10. Their contents of TiO_2, Al_2O_3, Cr_2O_3, MnO and CaO vary widely (0.0–0.27 wt%; 2.47–4.28 wt%; 0.35–0.68 wt%; 0.11–0.18 wt% and 0.29–0.97 wt%, respectively). Clinopyroxene compositions are in the range $En_{47.2\text{–}52.5}$, $Fs_{2.9\text{–}6.2}$, and $Wo_{41.4\text{–}47.8}$, with Mg# from 89.8 to 94.8. Their Cr_2O_3, Na_2O and TiO_2 contents vary between 0.83–1.57 wt%, 0.47–2.21 wt%, and 0.03–0.67 wt%, respectively. The spinel chromium numbers ($Cr\# = 100 \times Cr/(Cr + Al)$ in atomic units) vary from 14.3 to 33.9, and most of their Mg# range from 70.23 to 79.28, except for sample PM20-22 that give a lower value of 59.83. The variation of spinel Cr# and Mg# of coexisting olivine is shown in Fig. 2, together with southern South Africa peridotites (East Griqualand and Eastern Namaqualand) and the fields for cratonic and off-craton spinel peridotites defined by Janney et al. (2010) and references therein.

Sulfide analyses were possible for 6 peridotite samples; the results of which are presented in Supplementary Table 6. Mineral phases identified on interstitial and enclosed sulfides correspond to pentlandite (Pn), monosulfide solid solution (Mss) and chalcopyrite (Cp). Some sulfides are homogeneous grains while others include two or three phases (Supplementary Fig. 2). No compositional differences between enclosed and interstitial sulfide phases of the same type can be recognized.

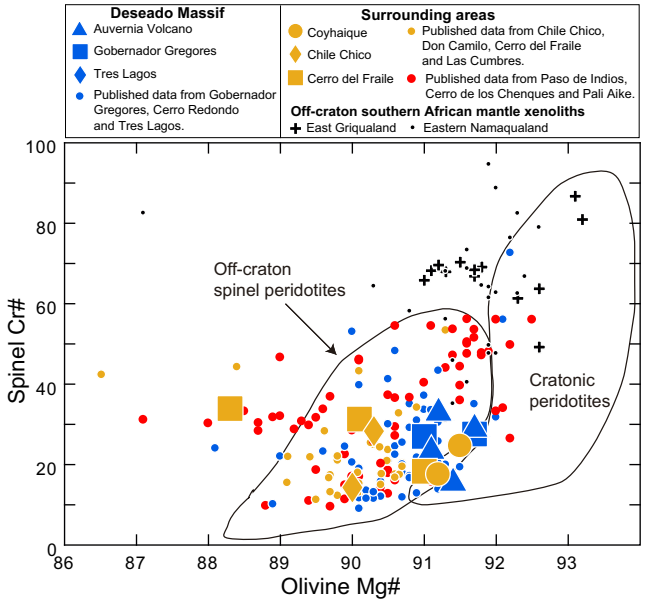

Fig. 2. Plot of spinel Cr# vs Mg# of coexisting olivine. Large symbols are samples from the present study and small symbols show published data. Tres Lagos: Rivalenti et al. (2004), Bjerg et al. (2005), Ntaflos et al. (2007), and Mundl et al. (2015); Gobernador Gregores: Aliani et al. (2009), Gorring and Kay (2000), Laurora et al. (2001), Rivalenti et al. (2004), Bjerg et al. (2005), and Mundl et al. (2015); Cerro Redondo: Schilling et al. (2005); Cerro del Fraile: Kilian and Stern (2002), Rivalenti et al. (2004), Wang et al. (2007), and Faccini et al. (2013); Cerro Clark: Dantas et al. (2009); Chile Chico: Schilling et al. (2008); Don Camilo: Mundl et al. (2015); Las Cumbres: Rivalenti et al. (2004); Pali AIke: Kempton et al. (1999), Bjerg et al. (2005), Wang et al. (2008), and Mundl et al. (2015); Paso de Indios: Rivalenti et al. (2004); Cerro de los Chenques: Rivalenti et al. (2007), Dantas et al. (2009). Peridotites from East Griqualand and Eastern Namaqualand, Southern Africa, are shown for comparison together with the fields for cratonic and off-craton spinel peridotites (Janney et al., 2010 and references there in).

Equilibrium temperatures were calculated using core mineral compositions and the two-pyroxene thermometer of Brey and Köhler (1990) at an assumed pressure of 15 kbar. Samples reflecting equilibrium conditions according to the criteria proposed by Putirka (2008) based on Fe-Mg exchange coefficients between ortho and clinopyroxenes, yield equilibrium temperatures from 850 to 1132 °C (Table 1).

5.2. Whole rock major and trace element compositions

Major and trace element data are given in Supplementary Table 7. Fig. 3 shows the variation of MgO versus Al_2O_3, SiO_2, CaO, FeO_{tot} (all Fe expressed as FeO), TiO_2, and Na_2O of the studied samples together with a large data set of Patagonian peridotites (n = 272, all expressed in weight percent and on a volatile-free basis). Bulk-rock Al_2O_3 and CaO contents of the studied samples lie within the relatively narrow ranges of 0.73–2.97 wt% and 0.66–2.64 wt%, respectively. The whole data set shows a negative correlation between Al_2O_3, SiO_2, CaO, FeO_{tot}, TiO_2, Na_2O with MgO. Such trends are usually attributed to different degrees of partial melt extraction from a fertile primitive mantle (e.g. Maaløe and Aoki, 1977; McDonough and Sun, 1995). The xenoliths from Auvernia volcano and Tres Lagos show relatively high MgO (>46 wt%) and low CaO (<1 wt%) contents compared to the rest of samples. Peridotites from Auvernia volcano also show some of the lowest Al_2O_3 contents (~0.7 wt%). Several of the published Gobernador

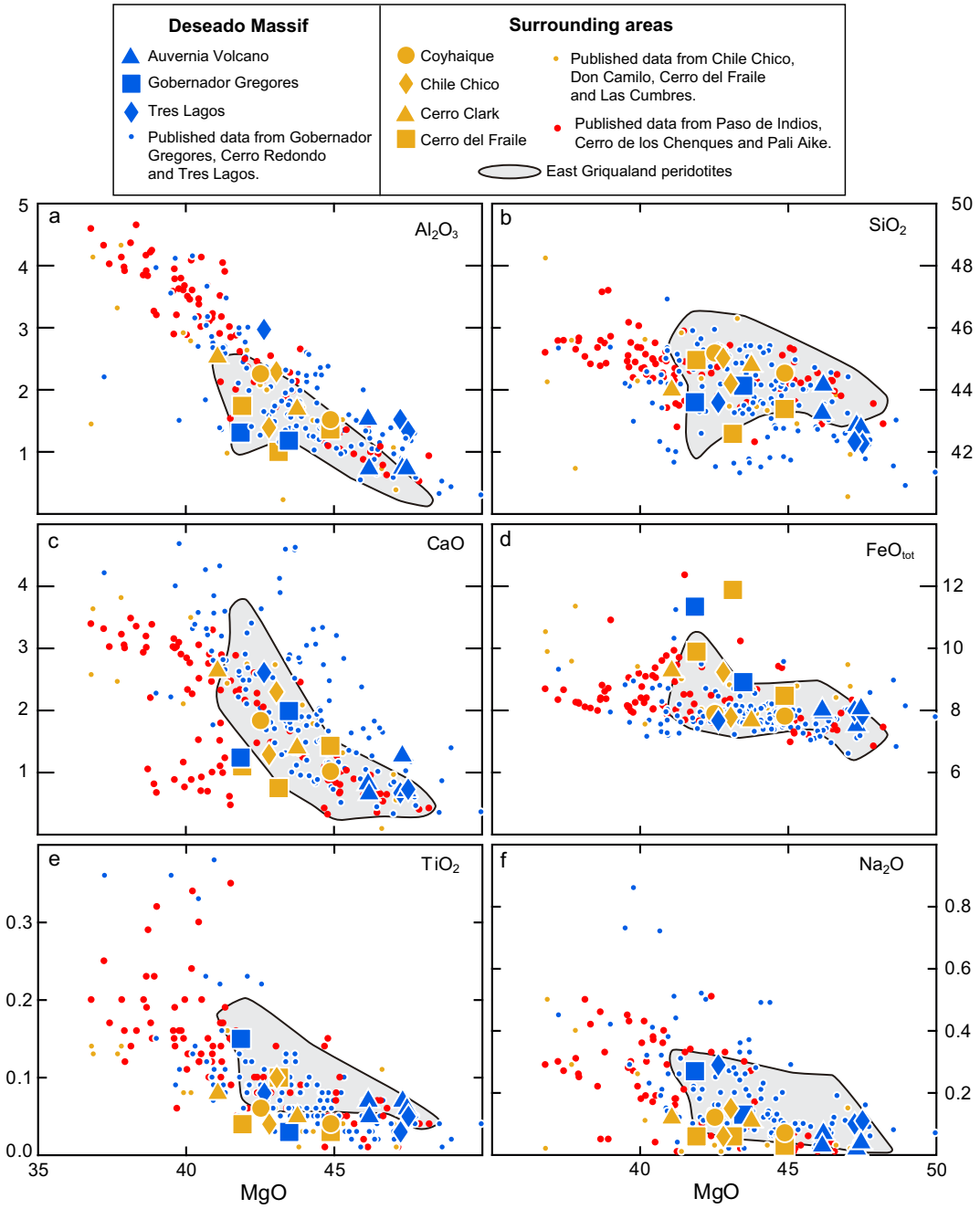

Fig. 3. Whole rock MgO vs (a) Al_2O_3, (b) SiO_2, (c) CaO, (d) FeO_{tot} (all Fe expressed as FeO), (e) TiO_2, and (f) Na_2O of Patagonian peridotites. All data expressed in weight percent and on a volatile-free basis. Large symbols represent samples of the present study while small symbols show other published data. Average values were plotted for samples with duplicate analyses (PM25-10, PN24-21, PM27B-2, PM23-21 and PM20-20). Tres Lagos: Rivalenti et al. (2004), Bjerg et al. (2005), Ntaflos et al. (2007), Pressi (2008) and Mundl et al. (2015); Cerro Redondo: Schilling et al. (2005); Gobernador Gregores: Gorring and Kay (2000), Laurora et al. (2001), Rivalenti et al. (2004), Aliani et al. (2009, 2004), Bjerg et al. (2005) and Mundl et al. (2015); Cerro del Fraile: Kilian and Stern (2002) and Wang (2007); Don Camilo: Mundl et al. (2015); Chile Chico: Niemeyer (1978); Las Cumbres: Muñoz (1981), Rivalenti et al. (2004); Paso de Indios: Rivalenti et al. (2004); Cerro de los Chenques: Rieck (2005) and Rivalenti et al. (2004); Pali Aike: Stern et al. (1999), Bjerg et al. (2005), Wang et al. (2008), Gervasoni et al. (2012) and Mundl et al. (2015). The range of compositions for the East Griqualand peridotites described by Janney et al. (2010) are shown for comparison by the shaded area.

Gregores peridotites exhibit considerably higher CaO contents for a given MgO that have been related to an intense modal and cryptic metasomatism (Gorring and Kay, 2000; Laurora et al., 2001), while some Pali Aike peridotites show significantly lower CaO content for a given MgO (Fig. 3c).

5.3. Re-Os isotopic compositions

The Re-Os isotopic results are given in Table 2 and shown in Fig. 4a along with previously published data for Patagonian and selected Southern African off-craton mantle xenoliths. Bulk-rock initial $^{187}Os/^{188}Os$ compositions (calculated back to the time of eruption indicated in Supplementary Table 1) range from 0.11389 to 0.12446, which are less radiogenic than the estimated value for the primitive mantle (0.1296) of Meisel et al. (2001). The only exception is sample PM23-21 from Gobernador Gregores that gives a superchondritic ratio of 0.13554, and the lowest single PGE contents varying from 0.01 to 0.72 ppb, with a total PGE content of ~1.8 ppb. These isotopic ratios lead to γOs values ranging from −12 to −3.9 for the subchondritic samples, and a value of

Table 2
Highly siderophile element concentrations (ppb), Re-Os isotopic results and model ages of Patagonian mantle xenoliths.

Locality	Sample	Os	Ir	Ru	Pt	Pd	Re	$^{187}Re/^{188}Os$	$^{187}Os/^{188}Os$	$^{187}Os/^{188}Os_{(i)}$	$\gamma Os_{(i)}$	T_{RD} (Ga)	T_{MA} (Ga)
Coyhaique													
	PM25-8	1.32	1.64	3.03	6.58	2.01	0.05	0.1594	0.12018	0.12002	−7.1	1.31	2.05
	PM25-10	1.78	4.39	5.93	5.63	0.78	0.02	0.0585	0.11718	0.11712	−9.3	1.70	1.96
Chile Chico													
	PM26-4	2.69	3.60	6.02	8.48	5.06	0.29	0.9851	0.12438	0.12370	−4.3	0.81	Future
	PM26-5	2.19	3.60	5.04	7.26	4.87	0.08	0.2669	0.12337	0.12319	−4.7	0.88	2.24
Cerro Clark													
	PM24-21	2.67	3.38	6.89	8.02	4.89	0.30	1.0069	0.12381	0.12361	−4.6	0.82	Future
	PM24-41	1.65	1.75	3.71	4.89	2.64	0.08	0.2710	0.12394	0.12389	−4.3	0.78	2.05
Auvernia Volcano													
	PM27A-9	3.34	2.73	10.20	3.29	0.28	0.09	0.2965	0.11469	0.11469	−11.5	2.02	6.13
	PM27B-1B	1.52	1.74	2.47	1.89	0.20	0.06	0.1963	0.11628	0.11627	−10.3	1.81	3.26
	PM27B-2	2.18	2.75	3.69	3.27	0.34	0.04	0.1452	0.11389	0.11389	−12.1	2.13	3.17
	PM27B-12B	1.56	1.51	2.37	2.11	0.58	0.07	0.2185	0.11791	0.11790	−9.0	1.59	3.16
Gobernador Gregores													
	PM23-3	3.19	3.95	8.55	8.42	1.17	0.01	0.0279	0.11589	0.11589	−10.6	1.86	1.99
	PM23-21	0.09	0.29	0.69	0.72	0.01	0.01	0.0235	0.13554	0.13554	4.6	Future	Future
Tres Lagos													
	PM21-1A	0.94	1.56	2.66	2.83	1.48	0.04	0.1439	0.12447	0.12446	−3.9	0.70	1.05
	PM21-6A	2.10	3.08	4.71	4.47	1.13	0.04	0.1197	0.11648	0.11647	−10.1	1.78	2.45
	PM21-9	1.84	3.20	5.38	4.94	1.46	0.03	0.0914	0.11483	0.11483	−11.4	2.00	2.53
Cerro del Fraile													
	PM20-8	0.80	0.90	1.31	5.25	1.05	0.07	0.2279	0.12366	0.12365	−4.6	0.81	1.70
	PM20-20	1.78	1.92	4.48	4.17	3.91	0.07	0.2343	0.12238	0.12237	−5.6	0.99	2.12
	PM20-22	1.00	1.52	2.73	3.23	0.16	0.04	0.1493	0.11455	0.11455	−11.6	2.04	3.08

$^{187}Os/^{188}Os$ are measured values, while $^{187}Os/^{188}Os_{(i)}$ are initial ratios calculated to the time of basalt eruption using the ages provided in Supplementary Table 1 and assuming a decay constant for ^{187}Re of 1.666×10^{-11} (Smoliar et al., 1996). The rhenium depletion (T_{RD}) and standard (T_{MA}) model ages and γOs are calculated assuming $^{187}Os/^{188}Os$ and $^{187}Re/^{188}Os$ values for the primitive upper mantle of 0.1296 and 0.4353, respectively (Meisel et al., 2001).

+4.6 for sample PM23-21 where γOs (Walker et al., 1989) is defined as:

$$\gamma Os = ((^{187}Os/^{188}Os)_{Sa}/(^{187}Os/^{188}Os)_{PM} - 1) \times 100$$

where "Sa" corresponds to sample and "PM" the primitive mantle value of Meisel et al. (2001). The $^{187}Re/^{188}Os$ ratios of most samples are lower than the estimated value for primitive mantle (0.4353) and range from 0.0235 to 0.2965, except for samples PM24-21 and PM26-4 that have considerably higher values (~1). Rhenium depletion ages (T_{RD}; Walker et al., 1989), calculated using the primitive mantle Re-Os parameters of Meisel et al. (2001), yield Neoproterozoic (0.7 Ga) to Paleoproterozoic (2.13 Ga) ages, while calculated T_{MA} model ages range from 1.05 to 6.13 Ga. There is no clear correlation between the Os isotopic compositions and $^{187}Re/^{188}Os$ (Fig. 4a). There is, however, a rough positive correlation between initial $^{187}Os/^{188}Os$ and bulk-rock Al_2O_3 content (Fig. 4b), as has been reported for other mantle xenolith suites (e.g. Handler et al., 1997; Meisel et al., 2001; Peslier et al., 2000).

In the central area of the DM, all xenoliths from the Auvernia volcano have $^{187}Os/^{188}Os$ ratios in the range 0.11389–0.11790; the lowest values reported for the massif. Consequently, these mantle samples have the oldest T_{RD} model ages ranging from 1.59 to 2.13 Ga. To the best of our knowledge, this is the eastern-most locality containing mantle xenoliths within the DM and surrounding regions. Two mantle xenoliths from Gobernador Gregores located approximately 100 km to the west-southwest of Auvernia volcano, also show unradiogenic Os isotopic compositions: one from our new data (0.11589), and the other (0.11679) from Schilling et al. (2008). In contrast, the four samples from this locality reported by Mundl et al. (2015) gave considerably higher ratios (0.12002–0.12631). Approximately 60 km to the south of Gobernador Gregores is Cerro Redondo, a volcanic neck located next to the Chico River, the geomorphological feature traditionally considered as marking the superficial southwestern margin of the DM. The three mantle xenoliths from Cerro Redondo reported by Schilling et al. (2008) gave relatively low $^{187}Os/^{188}Os$ isotopic ratios (0.11805–0.11979) corresponding to T_{RD} ages ranging from 1.34 to 1.57 Ga that are younger than peridotites from Auvernia volcano. Tres Lagos is approximately 80 km to the southwest of Cerro Redondo and the inferred southwestern margin of the DM. Our new data, together with those reported by Mundl et al. (2015), comprise four xenoliths with low $^{187}Os/^{188}Os$ ratios (0.11483–0.11733) and another three with higher values (0.12016–0.12504). So, considering that Auvernia volcano, Cerro Redondo, Gobernador Gregores, and Tres Lagos are located either within or less than 80 km from the DM, and they have similar and relatively low $^{187}Os/^{188}Os$ isotopic compositions, we interpret them to represent fragments derived from the Proterozoic lithospheric mantle section of the DM. Hence, the mantle samples from these localities were grouped as the "Deseado Massif" xenoliths (Figs. 2–6, and 8). Fig. 5c is a histogram of Re-depletion model ages for these xenoliths that show T_{RD} ages in the range 0.5–2.2 Ga, with a main peak from 1.5 to 2.0 Ga and an average of 1.5 ± 0.5 Ga (1σ, n = 20). A similar age distribution is observed for East Griqualand peridotites, eastern South Africa (1.48–2.56 Ga) as reported by Janney et al. (2010). The East Griqualand peridotites exhibit some older T_{RD} ages compared to the DM peridotites, and lack ages younger than 1.4 Ga, with an average of 1.9 ± 0.4 Ga (1σ, n = 14).

Compared to the results from xenolith localities within or near the DM, peridotites from the surrounding areas (Coyhaique, Chile Chico, Cerro Clark, and Cerro del Fraile) commonly have higher $^{187}Os/^{188}Os$ ratios (>0.120) and hence yield younger T_{RD} (<1.3 Ga) ages, similar to those of the North Patagonian Massif mantle xenoliths (Figs. 4 and 5). Only one sample from Cerro del Fraile and one from Coyhaique have lower $^{187}Os/^{188}Os$ isotopic ratios similar to those of the DM xenoliths (0.11455 and 0.11712, respectively). The mantle xenoliths from Don Camilo reported by Mundl et al. (2015) are located 25 km south of the Deseado River, which is considered to be the northern superficial boundary of the DM, consequently they should be considered to be derived from the

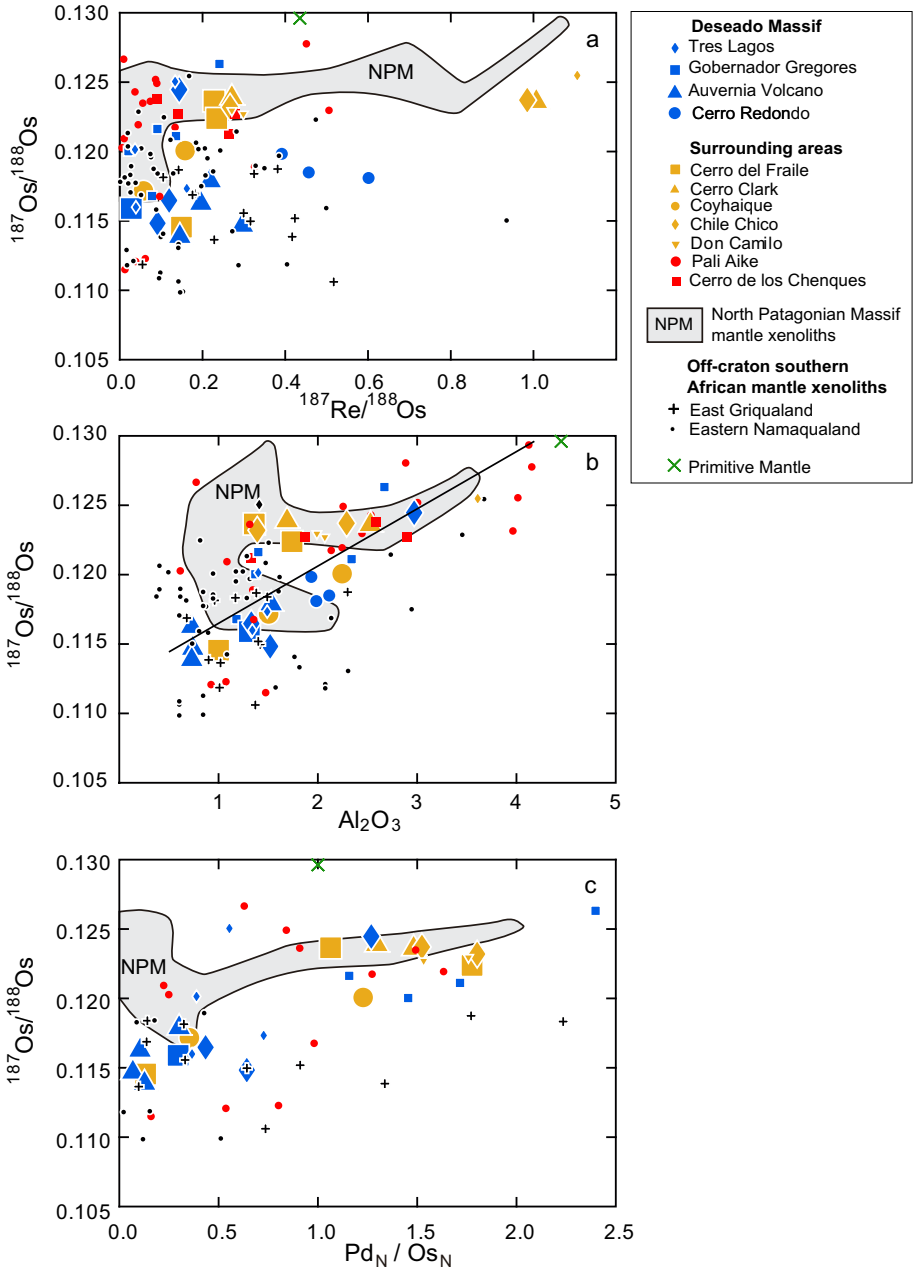

Fig. 4. Initial $^{187}Os/^{188}Os$ (calculated to the time of eruption) versus (a) $^{187}Re/^{188}Os$, (b) bulk-rock Al_2O_3 and (c) Pd_N/Os_N ratios (N = concentrations normalized to primitive mantle estimates of Becker et al., 2006) of Patagonian peridotites. Large symbols for samples from the present study and small symbols for previously published data from Stern et al. (1999), Schilling et al. (2008) and Mundl et al. (2015). NPM show the range of compositions for mantle xenoliths derived from the North Patagonian Massif reported by Schilling et al. (2008) and Mundl et al. (2016). Peridotites from East Griqualand and Eastern Namaqualand, Southern Africa, are also shown for comparison (Janney et al., 2010). Primitive mantle is from Meisel et al. (2001) (Re-Os) and McDonough and Sun (1995) (Al_2O_3). The regression line through all of the Deseado Massif data (n = 20, excluding sample PM23-21) is shown in (b).

lithospheric mantle of the DM according to geographic considerations. In contrast, based on their relative high $^{187}Os/^{188}Os$ isotopic compositions (0.12270–0.13267) compared to other DM mantle xenoliths and its proximity to the inferred boundary of the massif, we instead group them together with other localities from the surrounding areas of the DM (Figs. 2–6, and 8). This grouping is based on the Os isotope data, not the surface geographic boundaries of the DM, and thus assumes that the surface expressions used to define the borders of the DM do not necessarily coincide with the terrane boundaries at mantle depths.

Published Os isotopic data for mantle xenoliths from the Pali Aike volcanic field (Mundl et al., 2015; Schilling et al., 2008; Stern et al., 1999) are shown separately for comparison because they exhibit the widest range of Os isotopic compositions (0.11145–0.12930; Fig. 4) and hence T_{RD} ages of all Patagonian peridotites (0.0–2.5 Ga; Fig. 5b) including the oldest model ages (2.3–2.5 Ga) of southern South American mantle xenoliths (Mundl et al., 2015). The Pali Aike mantle rocks, together with those from Prahuaniyeu, are the only ones containing garnet in their mineral assemblage, corresponding to the deepest mantle rocks found in Patagonia. Most of the T_{RD} ages obtained for Pali Aike xenoliths range between 0.5 and 1.0 Ga (average = 1.0 ± 0.7 Ga, 1σ, n = 23). The Pali Aike suite shows a similar age distribution to Eastern Namaqualand peridotites, western

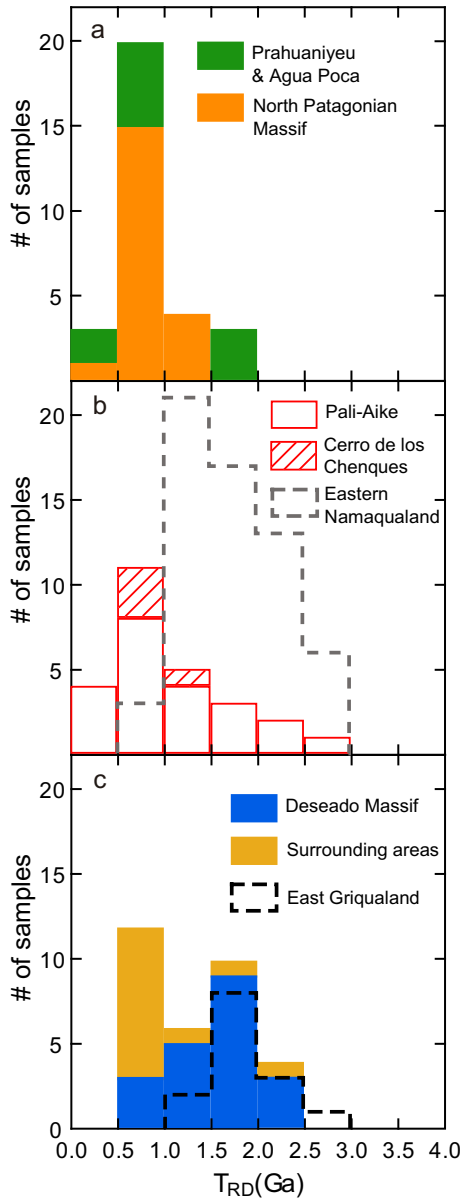

Fig. 5. Histograms of rhenium depletion model ages (T_{RD}) calculated for Patagonian peridotites. Same data sources as in Fig. 4: this study, Stern et al. (1999), Schilling et al. (2008) and Mundl et al. (2016, 2015). (a) Peridotites from the North Patagonian Massif show relatively young ages (0.0–1.5 Ga), peaking between 0.5 and 1.0 Ga, while peridotites from Prahuaniyeu and Agua Poca have similar young T_{RD} ages together with considerably older ages (1.5–2.0 Ga). (b) Pali Aike peridotites exhibit the widest range of ages of all Patagonian peridotites ranging from 0.0 to 2.5 Ga, with a similar main peak between 0.5 and 1.0 Ga, and similar T_{RD} distribution to the Eastern Namaqualand peridotites of Janney et al. (2010) but extending to younger ages. Cerro de los Chenques peridotites show similar T_{RD} ages to peridotites from the North Patagonian Massif. (c) Peridotites from the Deseado Massif (Auvernia volcano, Gobernador Gregores, Cerro Redondo and Tres Lagos) yield relatively old T_{RD} ages (0.5–2.5 Ga) with most samples in the range 1.5–2.0 Ga. A similar peak is observed for East Griqualand peridotites (Janney et al., 2010), which extend to slightly older T_{RD} ages compared to Deseado Massif peridotites, and do not show ages <1 Ga. Peridotites from the areas surrounding the DM (Coyhaique, Chile, Cerro Clark, Don Camilo and Cerro del Fraile) have T_{RD} ages mainly in the range 0.5–1.0 Ga, with some ages extending the range to 1.0–2.5 Ga.

South Africa, reported by Janney et al. (2010) but extends to younger ages (Eastern Namaqualand average = 1.6 ± 0.5 Ga, 1σ, n = 42). Cerro de los Chenques peridotites also show similar T_{RD} ages to peridotites from the North Patagonian Massif (Fig. 5a, b), with most samples in the range 0.5–1.0 Ga, and without ages older than 1.5 Ga (Schilling et al., 2008).

5.4. Highly siderophile element (HSE) concentrations

The highly siderophile element (HSE; PGE + Re) concentrations of the 18 studied samples are reported in Table 2. Rhenium contents range from 0.007 to 0.300 ppb, while Os concentrations range from 0.09 ppb (PM23-21) to 3.34 ppb (PM27A-9). The analyzed mantle xenoliths also exhibit variable contents of Ir (0.29–4.39 ppb), Ru (0.69–10.20 ppb), Pt (0.72–8.48 ppb) and Pd (0.01–5.06 ppb). The patterns of HSE contents normalized to the primitive upper mantle values of Becker et al. (2006) are shown on Fig. 6. Mantle xenoliths from Cerro Clark and Chile Chico have unfractionated PGE patterns. Samples from Auvernia volcano exhibit a strong depletion in palladium-group PGE (PPGE), with a relative enrichment in Re (Fig. 6). Xenoliths from Tres Lagos and Gobernador Gregores are depleted in Pd and Re, but not Pt. Samples from Cerro del Fraile and Coyhaique show variable patterns, some depleted in Pd and Re, other samples with flat patterns, and even some showing enrichments of Pt, Pd, and Re (Fig. 6). Samples with Pd_N/Os_N ratios <1 also show low $^{187}Os/^{188}Os$ ratios (<0.120), while samples with Pd_N/Os_N ratios > 1 yield higher Os isotopic ratios (>0.120), as shown on Fig. 4c (N indicate values normalized to primitive upper mantle estimates of Becker et al., 2006).

6. Discussion

6.1. Melt depletion ages of the Patagonian lithospheric mantle and their implications for the tectonic evolution of southern South America

The new Os isotopic data for mantle xenoliths presented here, combined with those previously published (Mundl et al., 2016, 2015; Schilling et al., 2008; Stern et al., 1999), confirm the hypothesis that the lithospheric mantle of the DM, southern Patagonia, was formed during the Paleo to Mesoproterozoic. The average of calculated T_{RD} ages is 1.5 ± 0.5 Ga (1σ, n = 20) for the DM mantle xenoliths (Auvernia volcano, Gobernador Gregores, Cerro Redondo and Tres Lagos). The T_{RD} ages of the xenoliths likely provide minimum estimates of the time of the melt depletion event that created the refractory peridotites sampled by the xenoliths. Many of the DM xenoliths have sufficiently low bulk-rock Al_2O_3 concentrations that the degree of melt extraction needed to reach these compositions likely reduced the Re/Os ratios of the residual peridotites to near zero, which is a requirement for the T_{RD} age to provide an accurate estimate of the timing of melt extraction (Walker et al., 1989). The average T_{RD} age for the DM xenoliths that have Al_2O_3 concentrations of 1 wt% or less is 1.99 ± 0.16 Ga (1σ, n = 3) (excluding sample PM23-21). For those samples with higher Al_2O_3 contents, the Re/Os ratio of the residual peridotite after melt extraction likely was not zero, which would lead the T_{RD} approach to underestimate the true timing of melt extraction. In such cases, one approach to estimate the true age of melt depletion is to extrapolate an observed correlation of Al_2O_3 vs $^{187}Os/^{188}Os$ to the Al_2O_3 content expected for a degree of melt extraction sufficient to lower the Re/Os ratio of the residual peridotite to zero (e.g. Reisberg and Lorand, 1995). Using this approach for the DM xenoliths leads to a $^{187}Os/^{188}Os \sim 0.1144$ at $Al_2O_3 = 0.5$ wt%, which translates to a model age of 2.07 Ga (Fig. 4b).

Samples with future or unrealistically old T_{MA} model ages (> 3 Ga) probably reflect Re addition, including infiltration by the host magma, subsequent to the main melting event associated with the stabilization of the subcontinental lithospheric mantle below southern Patagonia. This suggestion is consistent with the scattered distribution of $^{187}Os/^{188}Os$ and $^{187}Re/^{188}Os$ ratios (Fig. 4a), that can be explained by variable amounts of Re addition after the initial partial melt extraction events that determined the major element composition of these rocks.

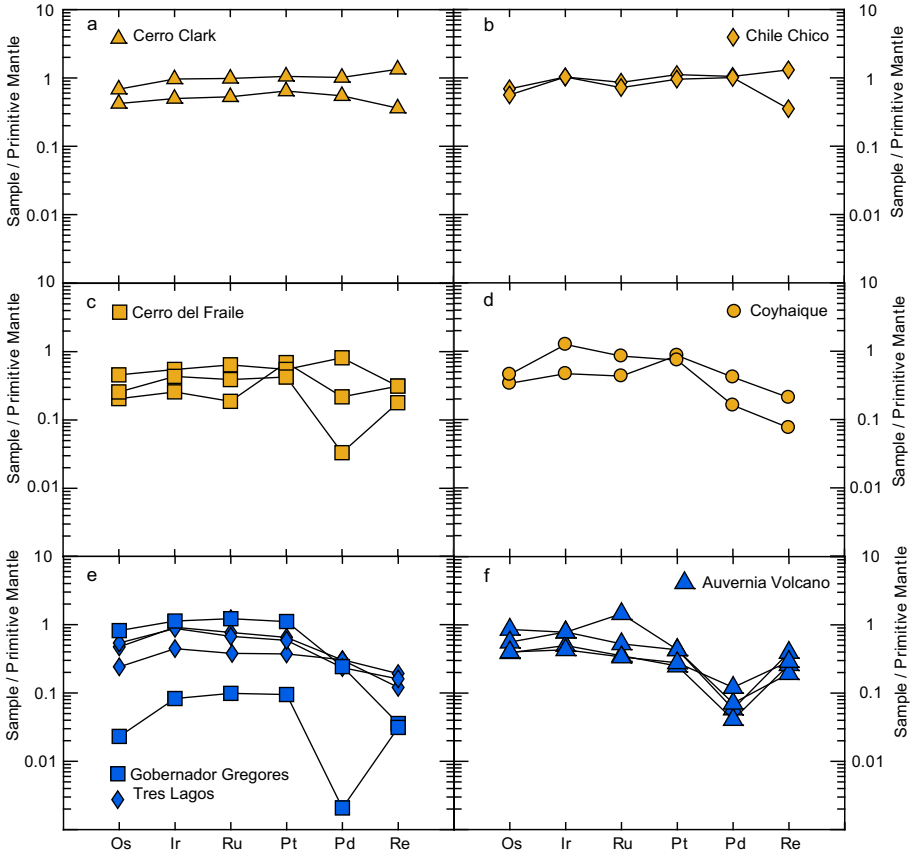

Fig. 6. Highly siderophile element patterns of Patagonian peridotites normalized to primitive upper mantle values of Becker et al. (2006). Cerro Clark (a) and Chile Chico (b) peridotites have relatively unfractionated HSE patterns while patterns for Tres Lagos and Gobernador Gregores samples (e) are variably depleted in Pt, Pd and Re relative to Os, Ir and Ru. Auvernia volcano peridotites (f) also show patterns depleted on Pt and Pd but with relatively high Re contents compared to Pd, what can be explained by a Re addition after an initial partial melting event. Peridotites from Cerro del Fraile (c) and Coyhaique (d) have both patterns: unfractionated HSE and variably depleted in Pd and Re.

Our results suggest that the estimated melt depletion age of the DM lithospheric mantle samples is significantly older than the available geochronological results (<0.6 Ga) for the very scarce crustal basement rocks exposed in the DM (Moreira et al., 2013; Pankhurst et al., 2003). The DM xenolith model ages also are considerably older than the average of model ages for samples of the surrounding localities Cerro de los Chenques, Coyhaique, Chile Chico, Cerro Clark, Don Camilo, and Cerro del Fraile (1.02 ± 0.4 Ga, 1σ, n = 16), and also from Pali Aike (1.0 ± 0.7 Ga, 1σ, n = 23). Nevertheless, some samples from Pali Aike give considerably older T_{RD} ages indicating a wider range of ages for melt extraction from the mantle beneath this locality. Several of the samples from areas surrounding the DM, however, have $^{187}Os/^{188}Os$ ratios within the range seen in modern abyssal peridotites (e.g. Snow and Reisberg, 1995), providing further support that these samples reflect relatively young additions to the continental lithospheric mantle.

According to reconstructions of Gondwana prior to the opening of the Atlantic Ocean, Patagonia was close to the Malvinas/Falkland Islands, and both were close to southeastern Africa (e.g. Marshall, 1994). Based on these paleogeographic considerations and the occurrence of Grenville-age continental rocks, the Malvinas/Falkland Islands have been interpreted as a microplate related to the eastern extension of the Namaqua-Natal Province (NNP). The NNP is a 100–500 km wide orogenic belt composed of a number of crustal subprovinces of distinct Paleo to Mesoproterozoic ages (2.2–1.0 Ga) and metamorphic grades bounded by tectonic discontinuities, that extends between the east and west coast of South Africa, around the southern margin of the Archean Kaapvaal craton (Hartnady et al., 1985; Thomas et al., 1994). The continuity of this Mesoproterozoic destructive plate margin has been traced via the Falkland Plateau and Falkland Islands, into the Ellsworth-Whitmore Mountains block, West Antarctica, and into western Dronning Maud Land in East Antarctica (Jacobs et al., 2008; Wareham et al., 1998). Near the southeast coast of South Africa, the basement of the eastern NNP is a Mesoproterozoic arc sequence, consisting primarily of granulite-facies tonalitic and granodioritic orthogneisses and amphibolite-grade metasediments having zircon U-Pb ages ranging from 1.0 to 1.3 Ga (Cornell, 1996; Eglington and Armstrong, 2003; McCourt et al., 2006). The lithospheric mantle of southeast Africa associated with 1.1 Ga continental crust was well characterized by the study of garnet and spinel bearing mantle xenoliths hosted in Mesozoic (194–150 Ma) kimberlites from East Griqualand performed by Janney et al. (2010). The East Griqualand mantle samples exhibit remarkably similar chemical characteristics to those reported from the DM, including major element (Fig. 3) and Os isotopic compositions and model ages (Figs. 4 and 5). Most T_{RD} ages of mantle xenoliths from East Griqualand (average of T_{RD} = 1.9 ± 0.4 Ga (1σ, n = 14)) and the DM range from 1.5 to 2.0 Ga, but the former also show some older ages and lack ages younger than 1.0 Ga as observed on the DM xenoliths. These differences suggest that the formation of the lithospheric mantle of southeast Africa started earlier than that of the DM, or that the former contain remnants of Paleoproterozoic to Archaean lithospheric mantle. The latter explanation is likely considering the proximity of the East Griqualand and the Lesotho kimberlite field (<100 km), whose mantle xenoliths predominantly yield Archean Re-Os model ages (Irvine et al., 2001).

Furthermore, the provenance ages of detrital zircon grains in metasedimentary rocks of the DM are typically Gondwanan with prominent ages of 550–750 Ma (Pampean and Brasiliano) and 1000–1200 Ma ('Grenvillian'), as well as a small component of 1750–2000 and 2550–2700 Ma (Hervé et al., 2003; Moreira et al., 2013; Pankhurst et al., 2003). We speculate that most of the Proterozoic zircons are likely derived from ancient basement rocks of the DM currently hidden under younger rocks or sedimentary cover, and not necessarily from other ancient continental regions of South America, southern South Africa or Antarctica as suggested previously by Hervé et al. (2003).

Another relevant observation is the chemical and isotopic similarity between the Pali Aike and Eastern Namaqualand mantle xenoliths, particularly their wide range of Al_2O_3 contents and $^{187}Os/^{188}Os$ ratios (Fig. 4b), and similar distribution of T_{RD} model ages (Fig. 5b). Again, the South African xenoliths include some samples with lower $^{187}Os/^{188}Os$ ratios (and hence, older T_{RD} model ages) than the South American counterpart, which exhibit the oldest T_{RD} ages (Paleoproterozoic) determined thus far for Patagonian mantle xenoliths (Mundl et al., 2015). This is noteworthy because the western NNP crustal basement related to the Eastern Namaqualand mantle xenoliths is composed dominantly of granulite- and amphibolite-facies supracrustal rocks and volcanic sequences with zircon U-Pb ages of 1.7–2.1 Ga (e.g. Eglington, 2006; Robb et al., 1999), intruded by younger gneissic granitoids with ages of 1.7–2.0 Ga and 1.1–1.3 Ga (Cornell et al., 1990; Pettersson et al., 2007; Robb et al., 1999). Most of the kimberlites in the Eastern Namaqualand cluster lie in a region where the crustal basement is predominantly of Paleoproterozoic age (~1.9 Ga), with a Mesoproterozoic metamorphic overprint (Schmitz and Bowring, 2004, 2001).

The available geochronological data can be integrated in a simple tectonic model where southern Patagonia, represented by the DM and its southern extension, and the corresponding continental shelf including the Malvinas/Falkland Islands, constitute a single continental block, referred to here as the Southern Patagonia-Malvinas Islands terrane. This continental block is linked to the Meso to Paleoproterozoic NNP and the formation of the Rodinia super continent. This terrane can also be correlated to the continental crust of the Shackleton Range, Antarctica, as proposed by Mundl et al. (2015), where similar Paleo and Mesoproterozoic crustal rocks have been identified (Will et al., 2009). Therefore, these new data complement the tectonic model proposed by Pankhurst et al. (2006) extending the formation age of southern Patagonia to the Paleo-Mesoproterozoic, and address the open question about its unknown extension to the southeast.

An intriguing fact is that the Nd model ages determined for continental rocks from northern and southern Patagonia are similar with prominent age peaks between 1000 and 1600 Ma (Martínez Dopico et al., 2011; Pankhurst et al., 2006, 2003) that are interpreted as the initial mantle extraction to form the continental source material (DePaolo et al., 1991). Moreover, the provenance ages recognized for detrital zircon grains in metasedimentary rocks in northern and southern Patagonia basement rocks are similar, including frequent Mesoproterozoic zircons (Chernicoff et al., 2013; Hervé et al., 2013, 2003; Moreira et al., 2013; Pankhurst et al., 2006). However, the NPM lithospheric mantle exhibits $^{187}Os/^{188}Os$ ratios similar to those of the modern convecting mantle. Possible remnants of the Mesoproterozoic lithospheric mantle root of the NPM have been identified only at Prahuaniyeu (Mundl et al., 2016; Schilling et al., 2008). From these observations, we infer that the continental crust of southern and northern Patagonia was formed mainly during the Paleo to Mesoproterozoic. Nevertheless, the original lithospheric mantle section of the NPM was almost completely removed possibly during the collision that occurred during the Carboniferous between the DM and the NPM, associated with northeasterly subduction. According to Pankhurst et al. (2006), this tectonic event was also responsible for the loss of the lower crustal section of the NPM.

Future studies that involve measurements of the Os isotopic compositions of widely dispersed mantle xenoliths as well as geochronological studies of crustal xenoliths will contribute to identify and determine the extent of ancient lithospheric provinces of Patagonia that are now covered by younger volcanic and sedimentary rocks.

6.2. Physical, chemical, and thermal structure of Patagonian lithospheric mantle

Important physical heterogeneities of the Patagonian lithosphere were recognized using estimates of the elastic thickness (T_e) of South America by Tassara et al. (2007). T_e is a proxy for lithospheric thickness that can be inverted from gravity anomalies and surface topography (e.g. Watts, 2001), and is a powerful independent estimate for the structure of the lithosphere that can be compared with our chemical and chronological results. Large T_e values are commonly found inside old, cold and thick cratonic regions whereas low values are associated with young tectonic regions affected by thermomechanical weakening associated with magmatism, fluid percolation, active deformation and/or possible removal of lithospheric mantle sections (e.g. Pérez-Gussinyé and Watts, 2005; Tassara et al., 2007; Watts, 2001). Fig. 7 shows a map of T_e for the studied region as computed using a wavelet formulation of the classical flexural isostatic analysis that considers satellite-derived gravity anomalies and topography/bathymetry (see details

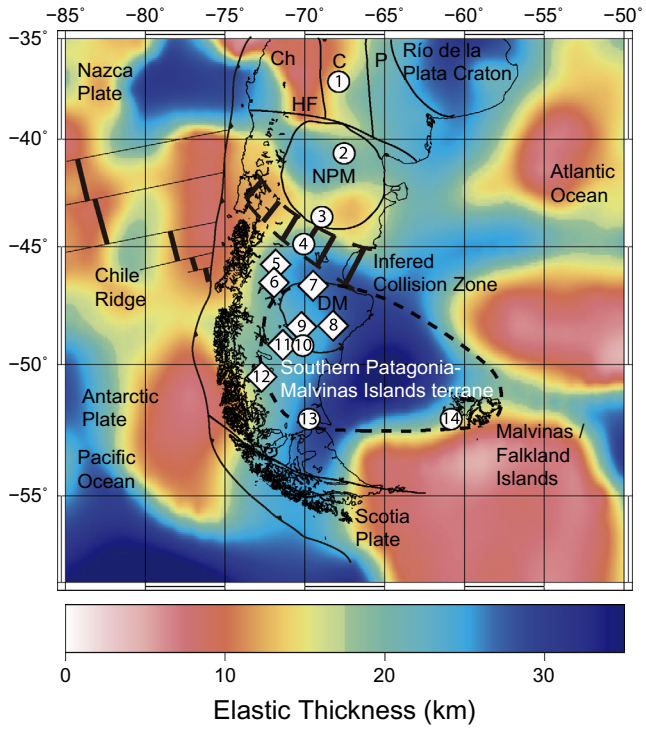

Fig. 7. Computed elastic thickness (T_e) map of southern South America by Tassara et al. (2007). Abbreviations and sample localities are detailed in Fig. 1. The maximum values of T_e, which are similar to those obtained for the Río de la Plata craton, reach 30–40 km in a region located right between the Deseado Massif and the Malvinas/Falkland Islands. These high T_e values suggest the presence of a thicker, more rigid and older lithospheric block compared to surrounding regions and strongly support the hypothesis of the integrated and independent Southern Patagonia-Malvinas Islands continental terrane (dashed line). The low T_e values (<20 km) on the southern margin of the North Patagonian Massif (NPM) are possibly related to thermomechanical weakening associated with the Carboniferous collision between the DM and the NPM.

in Tassara et al., 2007). The maximum values of T_e reach 30 to 40 km in a region located right between the DM and the Malvinas/Falkland Islands. This high T_e zone extends to the southwest, toward the southern edge of South America, passing through the area of the Pali Aike volcanic field, and also seems to continue to the east of the Malvinas/Falkland Islands, toward the Malvinas Plateau (Fig. 7). These high T_e values apparently reflect the presence of a thicker, colder, more rigid and older lithospheric block compared to surrounding regions and strongly support the hypothesis of the integrated and independent Southern Patagonia-Malvinas Islands continental terrane. To the north, on the southern margin of the North Patagonian Massif (NPM), there is a region of low T_e values (<20 km) that is partially coincident with the collision zone between the DM and the NPM (Fig. 7) that was associated with a northward subduction that occurred during the Carboniferous (Pankhurst et al., 2006). These particular physical characteristics could be the consequence of the thermomechanical weakening imposed by the tectonomagmatic activity in the previous convergent margin in this zone, and the subsequent extensive Early Permian crustal anatexis related to the post collisional slab break-off (Pankhurst et al., 2006). The relatively thin and weak (low viscosity) lithospheric mantle section of this region also could be related to high water concentration, as recognized by Dixon et al. (2004) in western North America but, in this case, without evidence for increased temperatures (see below). Considering this geophysical data, the hypothesis of a Devonian to mid Carboniferous "western magmatic arc" proposed by Ramos (2008) through the DM seems improbable. Additionally, the rotational model for the Malvinas Islands during the break-up of southern Gondwana (Adie, 1952; Marshall, 1994; Mitchell et al., 1986; Stone et al., 2009; Storey et al., 1999) is difficult to reconcile with our proposed model of an integrated Southern Patagonia-Malvinas Islands terrane, so the non-rotational model is preferred (Lawrence et al., 1999; Richards et al., 1996).

The composition of the Patagonian continental lithospheric mantle is examined by the available mineral and whole rock chemical data for mantle xenoliths carried to the surface by Eocene to recent alkali magmas (Figs. 2 and 3). The DM mantle xenoliths (Auvernia volcano, Gobernador Gregores, Cerro Redondo and Tres Lagos) exhibit notably more melt-depleted compositions compared to those derived from the surrounding areas (Cerro de los Chenques, Coyhaique, Chile Chico, Cerro Clark, Don Camilo, Cerro del Fraile and Pali Aike), reflecting, on average, higher degrees of partial melt extraction. The average whole rock Al_2O_3 concentration in the DM xenoliths (1.8 ± 0.8 wt%) is lower than that of xenoliths from surrounding regions (2.6 ± 0.8 wt%; data sources listed on Fig. 3), but the range overlaps. These chemical characteristics are relevant because more depleted mantle compositions yield less dense and more buoyant lithospheric mantle sections compared to more fertile ones (Boyd and McCallister, 1976; Jordan, 1978), and allow thick sections of depleted mantle to remain stable and attached to the overlying crust of similar age (James et al., 2004; Poudjom Djomani et al., 2001). Consequently, the more depleted composition of the DM lithospheric mantle results in a less dense and more buoyant lithospheric mantle section compared to those of the surrounding regions.

Furthermore, partial melt extraction also leaves the mantle lithosphere depleted in radioactive heat-producing trace elements (potassium, uranium, and thorium) and in water. The resulting combination of low temperature and low water content of mantle lithosphere will lead it to have considerably higher viscosity than warm and wet asthenospheric mantle (Dixon et al., 2004). To analyze the thermal characteristics of the southern Patagonian lithospheric mantle we recalculated the temperatures of equilibration at an assumed pressure of 15 kbar using available mineral compositions of mantle xenoliths (data sources on Fig. 2) and the two-pyroxene thermometer of Brey and Köhler (1990). Fig. 8 shows the histograms of temperature estimates of xenoliths from the DM and surrounding regions, excluding those samples that show chemical disequilibrium based on the criteria of Putirka (2008) that use Fe-Mg exchange coefficients between clinopyroxene and orthopyroxene. Nevertheless, no differences are recognized for temperatures of equilibration between the different lithospheric mantle domains in southern Patagonia identified using Os isotopic and bulk-rock compositions. This suggests a thermal homogenization of the continental lithosphere possibly caused by the intense magmatic activity that occurred during the Mesozoic and Cenozoic Eras. Given their similar temperatures, the more depleted lithospheric mantle compositions of the DM together with higher values of elastic thickness apparently reflect the presence of an older, thicker, and more buoyant and rigid lithospheric block compared to surrounding regions. The compositional buoyancy of the DM lithospheric mantle possibly increases its resistance to subduction and/or delamination, and can explain its positive relief compared to the surrounding areas.

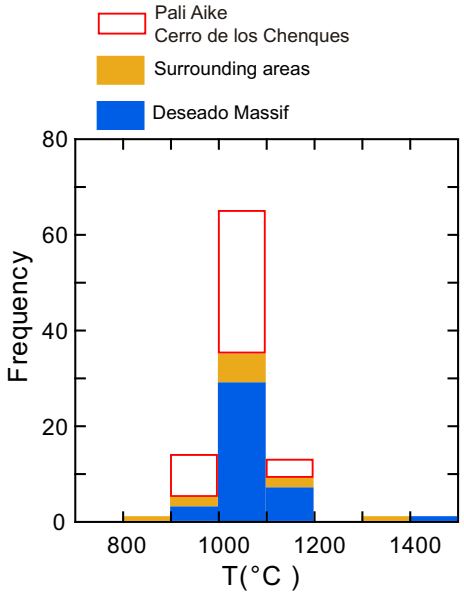

Fig. 8. Histograms of temperatures of equilibration calculated for Patagonian peridotites using the two-pyroxene thermometer of Brey and Köhler (1990) at an assumed pressure of 15 kbar. The Fe-Mg exchange coefficients between clinopyroxene and orthopyroxene were used to exclude samples that display chemical disequilibrium using the criteria proposed by Putirka (2008). The temperatures of equilibration calculated for the subcontinental lithospheric mantle of the Deseado Massif and surrounding regions are similar and range from 900 to 1200 °C with main peaks between 1000 and 1100 °C, suggesting that the Patagonian lithosphere has a homogeneous thermal structure.

6.3. Influence of Patagonian lithosphere heterogeneities on the formation of Jurassic metal deposits

The Jurassic extensional tectonic regime associated with Gondwana fragmentation and the opening of the Atlantic Ocean produced extensive stretching and melting of the Patagonian continental crust, resulting in the formation of the Chon Aike large igneous province that extends into west Antarctica (Pankhurst et al., 1998). In Patagonia, the volcanic products of this event are dominated by rhyolitic ignimbrites, which form a bimodal association with minor mafic and intermediate lavas. The geochemical signature of both silicic and intermediate rocks suggest that they were generated by partial melting of the lower continental crust (Gust et al., 1985; Kay et al., 1989; Pankhurst et al., 1998; Pankhurst and Rapela, 1995). The heat necessary to melt the lower

crust apparently came from the emplacement of voluminous mafic magmas beneath the continental crust (Gust et al., 1985; Pankhurst et al., 1998). The later stages of this Jurassic magmatism are related to the formation of important Au-Ag epithermal deposits in Patagonia (Fernández et al., 2008) that are particularly common in the DM (Echavarría et al., 2005; Giacosa et al., 2010; Moreira and Fernández, 2015; Schalamuk et al., 1997). Echavarría et al. (2005) argued that the basaltic and intermediate component of the bimodal magmatic suites may play a fundamental role in the supply of sulfur, chlorine, and even metals to the mineralizing hydrothermal fluids, as observed elsewhere (e.g. Hattori and Keith, 2001).

The apparently higher abundance of metals in the DM Jurassic magmas compared to those of the NPM may reflect the chemical

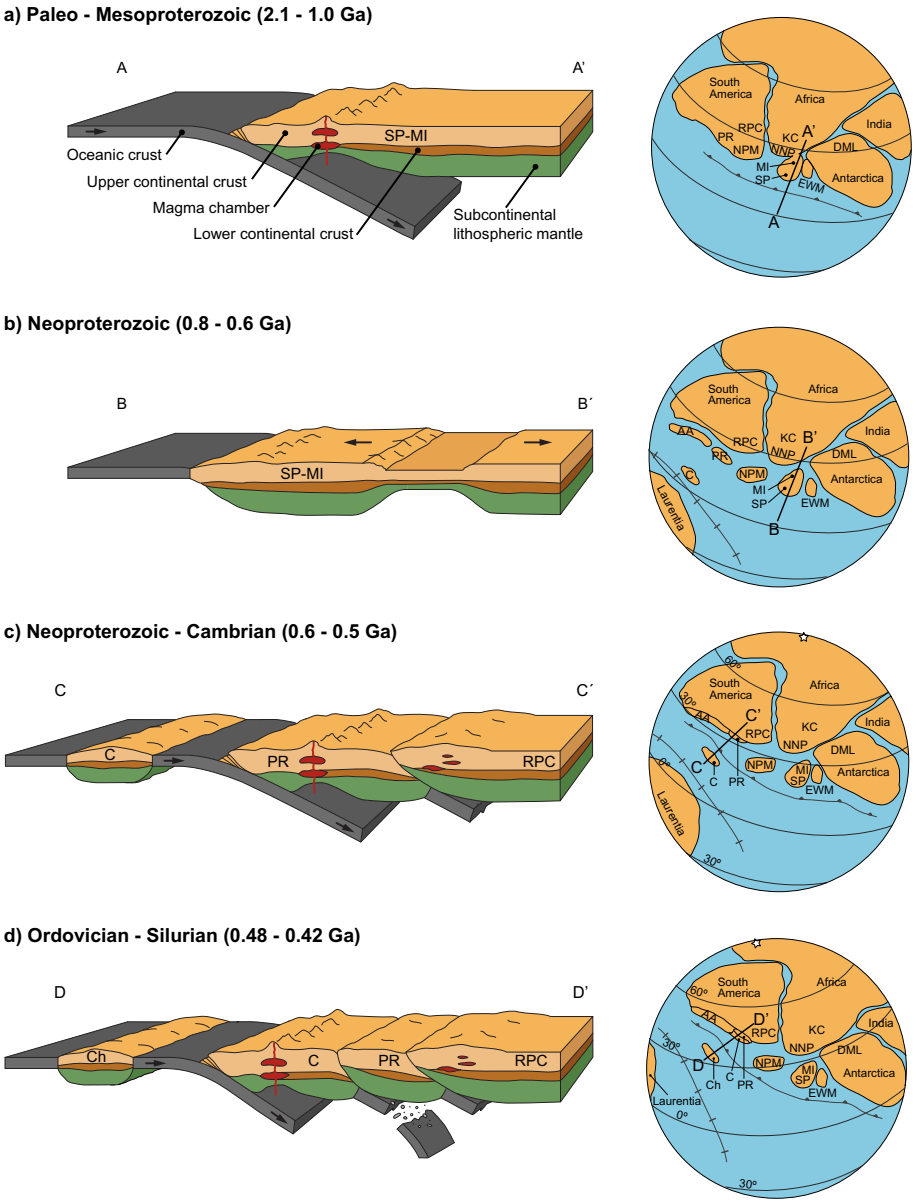

Fig. 9. Tectonic evolution model of Patagonia based on new and published geochemical and geophysical data. a) The formation of the Patagonian lithosphere started in the Paleo to Mesoproterozoic in a subduction setting, in part related to the Rodinia supercontinent and the Grenvillian orogeny. The melts generated during this event transported incompatible elements (including Re, Pd, Pt and Au) from the mantle wedge into the continental crust, producing a relatively melt-depleted lithospheric mantle and a metal-enriched lower crust. b) During the upper Neoproterozoic fragmentation of Rodinia, several continental blocks were detached from the main landmass (e.g. Southern Patagonia-Malvinas Island terrane, North Patagonian Massif and Pampian Ranges) to form a passive margin and sedimentary basins. c) The subduction process was reactivated on the western margin of Gondwana during the Cambrian. North of Patagonia, the Pampian Rages collided with the western margin of South America represented by the Río de la Plata craton. d) Middle Ordovician collision and amalgamation of the Cuyania terrane to the western margin of Gondwana. e) After the Upper Devonian collision of the Chilenia terrane to the western margin of Gondwana, a subduction zone was initiated between the North Patagonian Massif (upper block) and southern Patagonia. f) The later Carboniferous collision between southern Patagonia and the NPM produced extensive erosion and delamination of the lithospheric mantle and the lower crustal sections of the NPM, and the subsequent slab break-off and crustal anatexis until the Lower Triassic. g) The fragmentation of Gondwana started in the Lower Jurassic and was linked to continental crust extension and partial melting. The final stages of this magmatic event were associated with the formation of epithermal Au-Ag deposits derived from the partial melting of the lower crust. h) Numerous ore deposits were formed in the Upper Jurassic in the Deseado Massif, which had a fertile lower crust that supplied metals, while fewer ore deposits were formed in the North Patagonian Massif which had previously lost its lower crust. Abbreviations: AA, Arequipa-Antofalla terrane; AP, Antarctic Peninsula; C, Cuyania terrane; Ch, Chilenia terrane; DML, Dronning Maud Land; EWM, Ellsworth-Withmore Mountains terrane; KC, Kaapvaal craton; MEB, Maurice Ewing Bank; MI, Malvinas/Falkland Islands, NNP, Namaqua-Natal Province; PR, Pampian Ranges; RPC, Río de la Plata craton; SP, southern Patagonia. The location of the South Pole is shown by a star. This tectonic model was modified from the previous models of Cawood (2005), Jacobs et al. (2008), Keppie and Ramos (1999), Mpodozis and Ramos, (1989), Pankhurst et al. (2006), Rapela et al. (2003) and Torsvik and Cocks (2013).

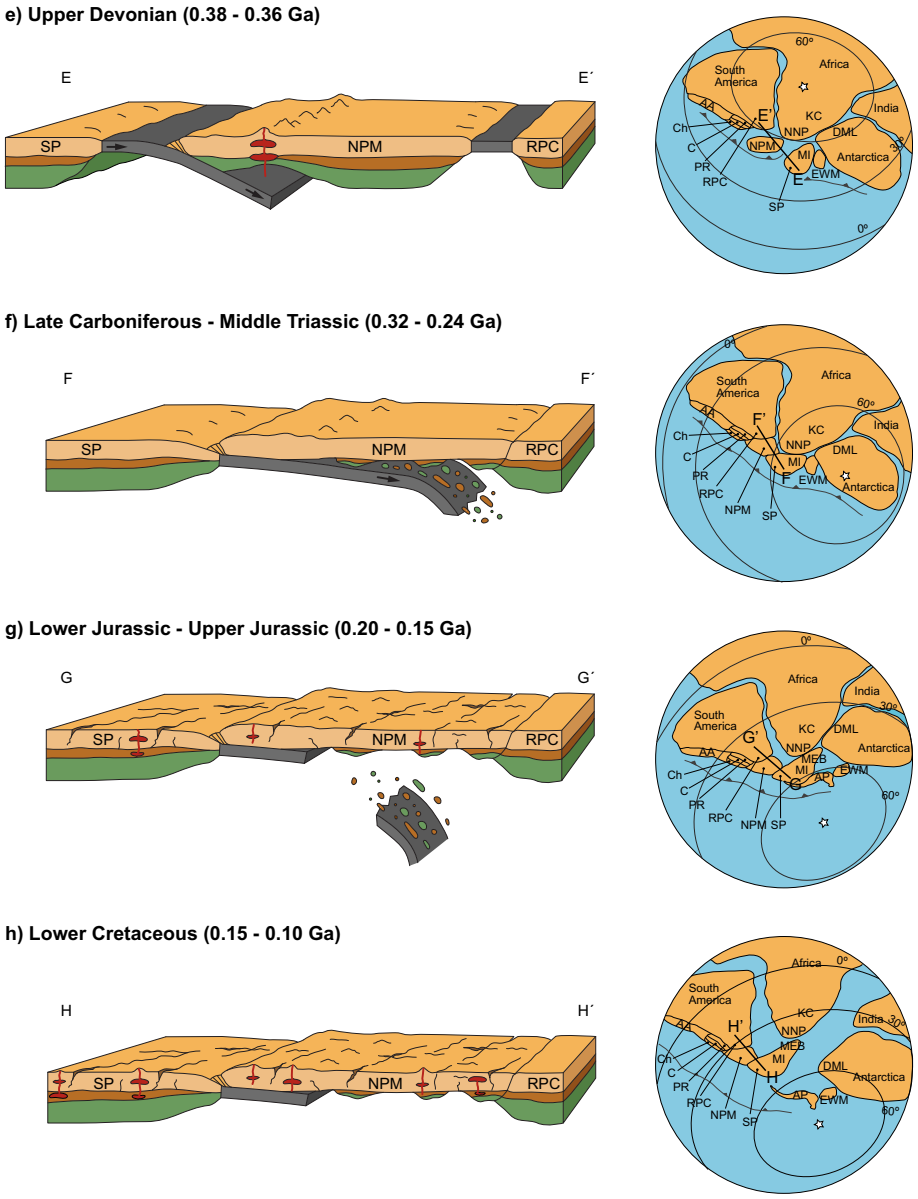

Fig. 9 (*continued*)

and physical differences of the respective lithospheres. The lower crustal sections, in particular, seem to play a key role as the main source of metals for the formation of the Jurassic ore deposits. We suggest that the relatively high degrees of partial melting that occurred during the formation of the Paleo to Mesoproterozoic Patagonian lithospheric mantle (including the DM and the NPM) produced mafic magmas that were relatively enriched in incompatible elements (including the precious metals Pd and Au) that accumulated and crystallized preferentially in the lower crust. At the same time, the subcontinental lithospheric mantle residue was strongly depleted in Pd, and probably in Au considering their similar behavior in the upper mantle. Later, the Carboniferous-Permian continental collision that occurred between the DM and the NPM related to north-easterly subduction, removed most of the Paleo to Mesoproterozoic lithospheric mantle section of the upper plate (NPM), replacing it with young asthenospheric convecting mantle. Remnants of the NPM Mesoproterozoic lithospheric mantle have been recognized only in Prahuaniyeu xenoliths (Mundl et al., 2015; Schilling et al., 2008). This hypothesis is supported by the notably lower average Pd concentration of the depleted DM mantle xenoliths (1.2 ± 1.0 ppb), compared to those of the surrounding regions (2.7 ± 1.1 ppb), and the relatively higher $^{187}Os/^{188}Os$ isotopic compositions of the NPM peridotites (excepting Prahuaniyeu). Pankhurst et al. (2006) infer that the subsequent Permian break-off of the subducted plate produced the partial delamination of the lower crust of the NPM. Additionally, this tectonic event caused voluminous and widespread silicic plutonism and volcanism throughout the Permian and into Triassic times (the Choiyoi volcanic province). Consequently, during the Jurassic tectonic extension and crustal anatexis, the DM lithosphere had a significant budget of precious metals (Pd, Au and Ag) accumulated in its lower crust, while the NPM lower crust was relatively depleted in metals resulting in the formation of considerably fewer ore deposits.

7. Conclusions

The geochemical data presented here, together with previously published Os isotopic measurements of mantle xenoliths and elas-

tic thickness estimates, contribute significantly to the comprehension of the controversial origin of Patagonia. The principal tectonic implications are shown schematically in Fig. 9.

We present here a summary of the main mantle melt extraction, metasomatic and erosional events related to the formation and evolution of the Patagonian lithosphere, together with their influence on the formation of precious metal deposits.

1. Peridotite mantle xenoliths from the Deseado Massif (DM), southern Patagonia, are residues of higher degrees of melt extraction compared to those from surrounding regions and display relatively low $^{187}Os/^{188}Os$ isotope ratios with an average T_{RD} model age of 1.5 ± 0.5 Ga (1σ, n = 20), resembling peridotites derived from East Griqualand (~1.1 Ga), southeastern Africa. This suggests that the DM lithospheric mantle was formed by relatively high degrees of partial melt extraction mainly during the Meso- to Paleoproterozoic (1.0–2.1 Ga), which is considerably earlier than the reported ages for the oldest exposed crustal basement rocks in this area (<0.6 Ga).
2. The presence of Paleoproterozoic continental domains incorporated into the southern Patagonian lithosphere can also be inferred by the similar chemical and Os isotopic compositions of Pali Aike peridotites located at the southern edge of South America that are comparable to those carried through Paleoproterozoic (~1.9 Ga) continental crust of Eastern Namaqualand, Southern Africa.
3. Southern Patagonia and the Malvinas/Falkland Islands constitute a single continental block characterized by relatively older, thicker, and more buoyant and rigid, but not colder lithospheric mantle compared to surrounding regions. This continental terrane is linked to the Namaqua-Natal Province and the formation of the Rodinia super continent. These new data address the origin of southern Patagonia, supporting the hypothesis of a parautochtonous origin and extending considerably its geological history to Meso- and even Paleoproterozoic.
4. The lithosphere of the North Patagonian Massif (NPM) also was formed during the Meso to Paleoproterozoic, however its ancient lithospheric mantle section was mostly eroded and replaced by younger convecting mantle. This tectonic process was probably triggered by the Carboniferous-Permian collision between the DM and the NPM related to a north-easterly subduction with subsequent slab break-off. Evidence for ancient lithospheric mantle relicts of the NPM have been found only at Prahuaniyeu.
5. The Late Paleozoic continental collision between north and south Patagonia responsible for the NPM lithospheric mantle erosion also caused partial delamination of its lower crust, inferred to be the main source of precious metals during the subsequent mineralization processes related to the Jurassic crustal stretching and anatexis. This could explain the fewer epithermal Au-Ag deposits discovered on the NPM compared to the DM, which is known as a precious metal rich province.

Acknowledgements

This work was supported by the Chilean National Commission for Scientific and Technological Research (CONICYT) through the Fondecyt project N°1100724 (Principal Investigator: M.E. Schilling), which is gratefully acknowledged. Analyses at DTM were supported by the Carnegie Institution for Science. Thanks to Michel Grégoire for microprobe analyses performed at the Paul Sabatier University and to Mary Horan for their kind assistance at the DTM isotope laboratory. Laura Hernández supported the microprobe analyses at the GEA Institute of Universidad de Concepción. Juan Bustamante performed the XRF analyses whereas Jorge Pizarro and Raúl Díaz prepared thin sections at the laboratory of SERNAGEOMIN. Isabel Guerrero is thanked for the creation of professional scientific illustrations that greatly benefited the paper. We thank Andrea Mundl and an anonymous reviewer for their constructive comments that helped to considerably improve this paper, and Randall Parrish for efficient editorial handling.

Appendix A. Supplementary data

Supplementary data associated with this article can be found, in the online version, at http://dx.doi.org/10.1016/j.precamres.2017.03.008.

References

Adie, R.J., 1952. The position of the Falkland Islands in a reconstruction of Gondwanaland. Geol. Mag. 89, 401. http://dx.doi.org/10.1017/S0016756800068102.
Aliani, P.A., Bjerg, E.A., Ntaflos, T., 2004. Evidencias de metasomatismo en el manto sublitosférico de Patagonia. Rev. la Asoc. Geol. Argentina 59, 539–555.
Aliani, P., Ntaflos, T., Bjerg, E., 2009. Origin of melt pockets in mantle xenoliths from southern Patagonia, Argentina. J. South Am. Earth Sci. 28, 419–428. http://dx.doi.org/10.1016/j.jsames.2009.04.009.
Aulbach, S., Griffin, W.L., Pearson, N.J., O'Reilly, S.Y., Kivi, K., Doyle, B.J., 2004. Mantle formation and evolution, Slave Craton: constraints from HSE abundances and Re–Os isotope systematics of sulfide inclusions in mantle xenocrysts. Chem. Geol. 208, 61–88. http://dx.doi.org/10.1016/j.chemgeo.2004.04.006.
Becker, H., Horan, M.F., Walker, R.J., Gao, S., Lorand, J.P., Rudnick, R.L., 2006. Highly siderophile element composition of the Earth's primitive upper mantle: constraints from new data on peridotite massifs and xenoliths. Geochim. Cosmochim. Acta 70, 4528–4550. http://dx.doi.org/10.1016/j.gca.2006.06.004.
Bjerg, E.A., Ntaflos, T., Kurat, G., Dobosi, G., Labudía, C.H., 2005. The upper mantle beneath Patagonia, Argentina, documented by xenoliths from alkali basalts. J. South Am. Earth Sci. 18, 125–145. http://dx.doi.org/10.1016/j.jsames.2004.09.002.
Boyd, F.R., McCallister, R.H., 1976. Densities of fertile and sterile garnet peridotites. Geophys. Res. Lett. 3, 509–512. http://dx.doi.org/10.1029/GL003i009p00509.
Brey, G.P., Köhler, T., 1990. Geothermobarometry in four-phase lherzolites II. New thermobarometers, and practical assessment of existing thermobarometers. J. Petrol. 31, 1353–1378. http://dx.doi.org/10.1093/petrology/31.6.1353.
Carlson, R.W., 2005. Application of the Pt–Re–Os isotopic systems to mantle geochemistry and geochronology. Lithos 82, 249–272. http://dx.doi.org/10.1016/j.lithos.2004.08.003.
Carlson, R.W., Moore, R.O., 2004. Age of the Eastern Kaapvaal mantle: Re-Os isotope data for peridotite xenoliths from the Monastery kimberlite. South Afr. J. Geol. 107, 81–90.
Carlson, R.W., Pearson, G.D., James, D.E., 2005. Physical, chemical, and chronological characteristics of continental mantle. Rev. Geophys. 43, RG1001. http://dx.doi.org/10.1029/2004RG000156.
Casquet, C., Pankhurst, R.J., Fanning, C.M., Baldo, E., Galindo, C., Rapela, C.W., González-Casado, J.M., Dahlquist, J.A., 2006. U-Pb SHRIMP zircon dating of Grenvillian metamorphism in Western Sierras Pampeanas (Argentina): correlation with the Arequipa-Antofalla craton and constraints on the extent of the Precordillera Terrane. Gondwana Res. 9, 524–529. http://dx.doi.org/10.1016/j.gr.2005.12.004.
Cawood, P.A., 2005. Terra Australis Orogen: Rodinia breakup and development of the Pacific and Iapetus margins of Gondwana during the Neoproterozoic and Paleozoic. Earth-Sci. Rev. 69, 249–279. http://dx.doi.org/10.1016/j.earscirev.2004.09.001.
Chernicoff, C.J., Zappettini, E.O., 2004. Geophysical evidence for terrane boundaries in South-Central Argentina. Gondwana Res. 7, 1105–1116. http://dx.doi.org/10.1016/S1342-937X(05)71087-X.
Chernicoff, C.J., Zappettini, E.O., Santos, J.O.S., McNaughton, N.J., Belousova, E., 2013. Combined U-Pb SHRIMP and Hf isotope study of the Late Paleozoic Yaminué Complex, Rio Negro Province, Argentina: implications for the origin and evolution of the Patagonia composite terrane. Geosci. Front. 4, 37–56. http://dx.doi.org/10.1016/j.gsf.2012.06.003.
Cingolani, C.A., Varela, R., 1976. Investigaciones geológicas y geocronológicas en el extremo sur de la isla Gran Malvina, sector Cabo Belgrano (Cabo Meredith), Islas Malvinas. VI Congr. Geológico Argentino, Bahía Blanca, 3, 457–473.
Conceição, R.V., Mallmann, G., Koester, E., Schilling, M., Bertotto, G.W., Rodriguez-Vargas, A., 2005. Andean subduction-related mantle xenoliths: isotopic evidence of Sr–Nd decoupling during metasomatism. Lithos 82, 273–287. http://dx.doi.org/10.1016/j.lithos.2004.09.022.
Cornell, D., 1996. Protolith interpretation in metamorphic terranes: a back-arc environment with Besshi-type base metal potential for the Quha Formation, Natal Province, South Africa. Precambr. Res. 77, 243–271. http://dx.doi.org/10.1016/0301-9268(95)00051-8.
Cornell, D.H., Griffin, G., Kroener, A., Humphreys, H., 1990. Age of origin of the polymetamorphosed Copperton Formation, Namaqua-Natal Province,

determined by single grain zircon Pb-Pb dating. South Afr. J. Geol. 93, 709–716.
Dantas, C., Grégoire, M., Koester, E., Conceição, R.V., Rieck, N., 2009. The lherzolite-websterite xenolith suite from Northern Patagonia (Argentina): evidence of mantle-melt reaction processes. Lithos 107, 107–120. http://dx.doi.org/10.1016/j.lithos.2008.06.012.
De la Cruz, R., Suárez, M., Belmar, M., Quiroz, D., Bell, M., 2003. Área Coihaique-Balmaceda, Región Aisén del General Carlos Ibáñez del Campo. Servicio Nacional de Geología y Minería, Carta Geológica de Chile, Serie Geología Básica, No. 80, 1 mapa escala 1:100.000.
DePaolo, D.J., Linn, A.M., Schubert, G., 1991. The continental crustal age distribution: methods of determining mantle separation ages from Sm-Nd isotopic data and application to the southwestern United States. J. Geophys. Res. 96, 2071. http://dx.doi.org/10.1029/90JB02219.
Dixon, J.E., Dixon, T.H., Bell, D.R., Malservisi, R., 2004. Lateral variation in upper mantle viscosity: role of water. Earth Planet. Sci. Lett. 222, 451–467. http://dx.doi.org/10.1016/j.epsl.2004.03.022.
Echavarría, L.E., Schalamuk, I.B., Etcheverry, R.O., 2005. Geologic and tectonic setting of Deseado Massif epithermal deposits, Argentina, based on El Dorado-Monserrat. J. South Am. Earth Sci. 19, 415–432. http://dx.doi.org/10.1016/j.jsames.2005.06.005.
Eglington, B.M., 2006. Evolution of the Namaqua-Natal Belt, southern Africa – a geochronological and isotope geochemical review. J. Afr. Earth Sci. 46, 93–111. http://dx.doi.org/10.1016/j.jafrearsci.2006.01.014.
Eglington, B., Armstrong, R.A., 2003. Geochronological and isotopic constraints on the Mesoproterozoic Namaqua-Natal Belt: evidence from deep borehole intersections in South Africa. Precambr. Res. 125, 179–189. http://dx.doi.org/10.1016/S0301-9268(02)00199-7.
Espinoza, F., 2003. Petrología y geoquímica de los basaltos cenozoicos de la meseta Chile Chico, 46° 35′-46°47′S – 71°46′-72°02′W, XI Región de Aysén, Chile. Universidad de Chile.
Faccini, B., Bonadiman, C., Coltorti, M., Grégoire, M., Siena, F., 2013. Oceanic material recycled within the sub-Patagonian lithospheric mantle (Cerro del Fraile, Argentina). J. Petrol. 54, 1211–1258. http://dx.doi.org/10.1093/petrology/egt010.
Fernández, R.R., Blesa, A., Moreira, P., Echeveste, H., Mykietiuk, K., De Palomera, P.A., Tessone, M., 2008. Los depósitos de oro y plata vinculados al magmatismo jurásico de la patagonia: Revisión y perspectivas para la exploración. Rev. la Asoc. Geol. Argentina 63, 665–681.
Frutos, J., Tobar, A., 1975. Evolution of the southwestern continental margin of South America. In: Campbell, K.S.W. (Ed.), III International Gondwana Symposium. Australian National University Press, Canberra, pp. 565–578.
Gervasoni, F., Conceição, R.V., Jalowitzki, T.L.R., Schilling, M.E., Orihashi, Y., Nakai, S., Sylvester, P., 2012. Heterogeneidades do manto litosférico subcontinental no extremo sul da placa sul-americana: Influência da subducção atual e interações litosfera-astenosfera sob o campo vulcânico de Pali Aike. Pesqui. em Geociencias 39, 269–285.
Giacosa, R., Zubia, M., Sánchez, M., Allard, J., 2010. Meso-Cenozoic tectonics of the southern Patagonian foreland: structural evolution and implications for Au–Ag veins in the eastern Deseado Region (Santa Cruz, Argentina). J. South Am. Earth Sci. 30, 134–150. http://dx.doi.org/10.1016/j.jsames.2010.09.002.
Gorring, M.L., Kay, S.M., 2000. Carbonatite metasomatized peridotite xenoliths from southern Patagonia: implications for lithospheric processes and Neogene plateau magmatism. Contrib. Mineral. Petrol. 140, 55–72. http://dx.doi.org/10.1007/s004100000164.
Gorring, M.L., Kay, S., 2001. Mantle processes and sources of Neogene slab window magmas from southern Patagonia, Argentina. J. Petrol. 42, 1067–1094. http://dx.doi.org/10.1093/petrology/42.6.1067.
Gorring, M.L., Kay, S.M., Zeitler, P.K., Ramos, V.A., Rubiolo, D., Fernandez, M.I., Panza, J.L., 1997. Neogene Patagonian plateau lavas: continental magmas associated with ridge collision at the Chile Triple Junction. Tectonics 16, 1–17. http://dx.doi.org/10.1029/96TC03368.
Griffin, W.L., O'Reilly, S.Y., Ryan, C.G., 1999. The composition and origin of sub-continental lithospheric mantle. In: Mantle Petrology: Field Observations and High-Pressure Experimentation. Spec. Publ. Geochem. Soc. No. 6, pp. 13–45.
Griffin, W., O'Reilly, S., Abe, N., Aulbach, S., Davies, R., Pearson, N., Doyle, B., Kivi, K., 2003. The origin and evolution of Archean lithospheric mantle. Precambr. Res. 127, 19–41. http://dx.doi.org/10.1016/S0301-9268(03)00180-3.
Griffin, W., Graham, S., O'Reilly, S.Y., Pearson, N., 2004. Lithosphere evolution beneath the Kaapvaal Craton: Re–Os systematics of sulfides in mantle-derived peridotites. Chem. Geol. 208, 89–118. http://dx.doi.org/10.1016/j.chemgeo.2004.04.007.
Griffin, W.L., O'Reilly, S.Y., Afonso, J.C., Begg, G.C., 2009. The composition and evolution of lithospheric mantle: a re-evaluation and its tectonic implications. J. Petrol. 50, 1185–1204. http://dx.doi.org/10.1093/petrology/egn033.
Gust, D.A., Biddle, K.T., Phelps, D.W., Uliana, M.A., 1985. Associated middle to late Jurassic volcanism and extension in southern South America. Tectonophysics 116, 223–253. http://dx.doi.org/10.1016/0040-1951(85)90210-0.
Handler, M.R., Bennett, V.C., Esat, T.M., 1997. The persistence of off-cratonic lithospheric mantle: Os isotopic systematics of variably metasomatised southeast Australian xenoliths. Earth Planet. Sci. Lett. 151, 61–75. http://dx.doi.org/10.1016/S0012-821X(97)00118-0.
Hanghøj, K., Kelemen, P., Bernstein, S., Blusztajn, J., Frei, R., 2001. Osmium isotopes in the Wiedemann Fjord mantle xenoliths: a unique record of cratonic mantle formation by melt depletion in the Archaean. Geochem. Geophys. Geosyst. 2. http://dx.doi.org/10.1029/2000GC000085.
Hartnady, C., Joubert, P., Stowe, C., 1985. Proterozoic crustal evolution in southwestern Africa. Episodes 8, 236–244.
Hattori, K.H., Keith, J.D., 2001. Contribution of mafic melt to porphyry copper mineralization: evidence from Mount Pinatubo, Philippines, and Bingham Canyon, Utah, USA. Miner. Deposita 36, 799–806. http://dx.doi.org/10.1007/s001260100209.
Hervé, F., Fanning, C.M., Pankhurst, R.J., 2003. Detrital zircon age patterns and provenance of the metamorphic complexes of southern Chile. J. South Am. Earth Sci. 16, 107–123. http://dx.doi.org/10.1016/S0895-9811(03)00022-1.
Hervé, F., Calderón, M., Fanning, C.M., Pankhurst, R.J., Godoy, E., 2013. Provenance variations in the Late Paleozoic accretionary complex of central Chile as indicated by detrital zircons. Gondwana Res. 23, 1122–1135. http://dx.doi.org/10.1016/j.gr.2012.06.016.
Homovc, J.F., Constantini, L., 2001. Hydrocarbon exploration potential within intraplate shear-related depocenters: Deseado and San Julian basins, southern Argentina. Am. Assoc. Pet. Geol. Bull. 85, 1795–1816.
Irvine, G.J., Pearson, D.G., Carlson, R.W., 2001. Lithospheric mantle evolution of the Kaapvaal Craton: a Re-Os isotope study of peridotite xenoliths from Lesotho kimberlites. Geophys. Res. Lett. 28, 2505–2508. http://dx.doi.org/10.1029/2000GL012411.
Irvine, G., Pearson, D.G., Kjarsgaard, B.A., Carlsonc, R.W., Kopylova, M.G., Dreibus, G., 2003. A Re–Os isotope and PGE study of kimberlite-derived peridotite xenoliths from Somerset Island and a comparison to the Slave and Kaapvaal cratons. Lithos 71, 461–488. http://dx.doi.org/10.1016/S0024-4937(03)00126-9.
Jacobs, J., Thomas, R.J., Armstrong, R.A., Henjes-Kunst, F., 1999. Age and thermal evolution of the Mesoproterozoic Cape Meredith Complex, West Falkland. J. Geol. Soc. London 156, 917–928. http://dx.doi.org/10.1144/gsjgs.156.5.0917.
Jacobs, J., Pisarevsky, S., Thomas, R.J., Becker, T., 2008. The Kalahari Craton during the assembly and dispersal of Rodinia. Precambr. Res. 160, 142–158. http://dx.doi.org/10.1016/j.precamres.2007.04.022.
Jalowitzki, T., Sumino, H., Conceição, R.V., Orihashi, Y., Nagao, K., Bertotto, G.W., Balbinot, E., Schilling, M.E., Gervasoni, F., 2016. Noble gas composition of subcontinental lithospheric mantle: an extensively degassed reservoir beneath Southern Patagonia. Earth Planet. Sci. Lett. 450, 263–273. http://dx.doi.org/10.1016/j.epsl.2016.06.034.
James, D.E., Boyd, F.R., Schutt, D., Bell, D.R., Carlson, R.W., 2004. Xenolith constraints on seismic velocities in the upper mantle beneath southern Africa. Geochem. Geophys. Geosyst. 5. http://dx.doi.org/10.1029/2003GC000551.
Janney, P.E., Shirey, S.B., Carlson, R.W., Pearson, D.G., Bell, D.R., Le Roex, A.P., Ishikawa, A., Nixon, P.H., Boyd, F.R., 2010. Age, composition and thermal characteristics of South African off-craton mantle lithosphere: evidence for a multi-stage history. J. Petrol. 51, 1849–1890. http://dx.doi.org/10.1093/petrology/egq041.
Jordan, T.H., 1978. Composition and development of the continental tectosphere. Nature 274, 544–548. http://dx.doi.org/10.1038/274544a0.
Kay, S.M., Ramos, V.A., Mpodozis, C., Sruoga, P., 1989. Late Paleozoic to Jurassic silicic magmatism at the Gondwana margin: analogy to the Middle Proterozoic in North America? Geology 17, 324. http://dx.doi.org/10.1130/0091-7613(1989)017<0324:LPTJSM>2.3.CO;2.
Kay, S.M., Orrell, S., Abbruzzi, J.M., 1996. Zircon and whole rock Nd-Pb isotopic evidence for a Grenville age and a Laurentian origin for the basement of the Precordillera in Argentina. J. Geol. 104, 637–648. http://dx.doi.org/10.1086/629859.
Keidel, J., 1925. Sobre el desarollo paleogeográfico del las grandes unidades geológicas de la Argentina. Sociedad Argentina de Estudios Geológicos GAEA, pp. 251–312.
Kempton, P.D., Lopez-Escobar, L., Hawkesworth, C.J., Pearson, G., Ware, A.J., 1999. Spinel ± garnet lherzolite xenoliths from Pali Aike: Part 1. Petrography, mineral chemistry and geothermobarometry. In: Gurney, J.J., Gurney, J.L., Pascoe, M.D., Richardson, S.H. (Eds.), Proceedings of the 7th International Kimberlite Conference. Red wood Design, Cape Town, pp. 403–414.
Keppie, J.D., Ramos, V.A., 1999. Odyssey of terranes in the Iapetus and Rheic oceans during the Paleozoic. In: Special Paper 336: Laurentia-Gondwana Connections Before Pangea. Geological Society of America, pp. 267–276. http://dx.doi.org/10.1130/0-8137-2336-1.267.
Kilian, R., Stern, C.R., 2002. Constraints on the interaction between slab melts and the mantle wedge from adakitic glass in peridotite xenoliths. Eur. J. Mineral. 14, 25–36. http://dx.doi.org/10.1127/0935-1221/2002/0014-0025.
König, M., Jokat, W., 2006. The Mesozoic breakup of the Weddell Sea. J. Geophys. Res. Solid Earth 111, 1–28. http://dx.doi.org/10.1029/2006JB004035.
Kostadinoff, J., Gregori, D.A., Raniolo, L.A., 2005. Configuración geofísica-geológica del sector norte de la provincia de Río Negro. Rev. la Asoc. Geol. Argentina 60, 368–376.
Laurora, A., Mazzucchelli, M., Rivalenti, G., Vannucci, R., Zanetti, A., Barbieri, M.A., Cingolan, C.A., 2001. Metasomatism and melting in carbonated peridotite xenoliths from the mantle wedge: the Gobernador Gregores case (Southern Patagonia). J. Petrol. 42, 69–87. http://dx.doi.org/10.1093/petrology/42.1.69.
Lawrence, S.R., Johnson, M., Tubb, S.R., Marshallsea, S.J., 1999. Tectono-stratigraphic evolution of the North Falkland region. Geol. Soc. London, Spec. Publ. 153, 409–424. http://dx.doi.org/10.1144/GSL.SP.1999.153.01.25.
Maaløe, S., Aoki, K., 1977. The major element composition of the upper mantle estimated from the composition of lherzolites. Contrib. Mineral. Petrol. 63, 161–173. http://dx.doi.org/10.1007/BF00398777.
Marshall, J.E.A., 1994. The Falkland Islands: a key element in Gondwana paleogeography. Tectonics.
Martínez Dopico, C.I., López de Luchi, M.G., Rapalini, A.E., Kleinhanns, I.C., 2011. Crustal segments in the North Patagonian Massif, Patagonia: an integrated

perspective based on Sm–Nd isotope systematics. J. South Am. Earth Sci. 31, 324–341. http://dx.doi.org/10.1016/j.jsames.2010.07.009.
McCourt, S., Armstrong, R.A., Grantham, G.H., Thomas, R.J., 2006. Geology and evolution of the Natal belt, South Africa. J. Afr. Earth Sci. 46, 71–92. http://dx.doi.org/10.1016/j.jafrearsci.2006.01.013.
McDonough, W.F., Sun, S.-s., 1995. The composition of the Earth. Chem. Geol. 120, 223–253. http://dx.doi.org/10.1016/0009-2541(94)00140-4.
Meisel, T., Walker, R.J., Irving, A.J., Lorand, J.-P., 2001. Osmium isotopic composition of mantle xenoliths: a global perspective. Geochim. Cosmochim. Acta 65, 1311–1323.
Mitchell, C., Taylor, G.K., Cox, K.G., Shaw, J., 1986. Are the Falkland Islands a rotated microplate? Nature 319, 131–134. http://dx.doi.org/10.1038/319131a0.
Moreira, P., Fernández, R.R., 2015. La Josefina Au–Ag deposit (Patagonia, Argentina): a Jurassic epithermal deposit formed in a hot spring environment. Ore Geol. Rev. 67, 297–313. http://dx.doi.org/10.1016/j.oregeorev.2014.12.012.
Moreira, P., Fernández, R., Hervé, F., Fanning, C.M., Schalamuk, I.A., 2013. Detrital zircons U-Pb SHRIMP ages and provenance of La Modesta Formation, Patagonia Argentina. J. South Am. Earth Sci. 47, 32–46. http://dx.doi.org/10.1016/j.jsames.2013.05.010.
Mpodozis, C., Ramos, V.A., 1989. The Andes of Chile and Argentina. In: Ericksen, G.E., Cañas, M.T., Reinemund, J.A. (Eds.), Geology of the Andes and Its Relation to Hydrocarbon and Energy Resources. Circum-Pacific Council for Energy and Hydrothermal Resources Circum-Pacific Council for Energy and Hydrothermal Resources. American Association of Petroleum Geologists, Earth Science Series, Houston, Texas, pp. 59–90.
Mundl, A., Ntaflos, T., Ackerman, L., Bizimis, M., Bjerg, E.A., Hauzenberger, C.A., 2015. Mesoproterozoic and Paleoproterozoic subcontinental lithospheric mantle domains beneath southern Patagonia: isotopic evidence for its connection to Africa and Antarctica. Geology 43, 39–42. http://dx.doi.org/10.1130/G36344.1.
Mundl, A., Ntaflos, T., Ackerman, L., Bizimis, M., Bjerg, E.A., Wegner, W., Hauzenberger, C.A., 2016. Geochemical and Os–Hf–Nd–Sr isotopic characterization of North Patagonian Mantle Xenoliths: implications for extensive melt extraction and percolation processes. J. Petrol. 57, 685–715. http://dx.doi.org/10.1093/petrology/egv048.
Muñoz, J., 1981. Inclusiones ultramáficas del manto superior en meseta Las Vizcachas, Ultima Esperanza, Magallanes, Chile. Rev. Geol. Chile 13–14, 63–78.
Niemeyer, H., 1978. Nódulos máficos y ultramáficos en basaltos alcalinos de la meseta de Buenos Aires, Lago General Carrera, provincia de Aysen, Chile. Rev. la Asoc. Geol. Argentina 33, 63–75.
Ntaflos, T., Bjerg, E.A., Labudia, C.H., Kurat, G., 2007. Depleted lithosphere from the mantle wedge beneath Tres Lagos, southern Patagonia, Argentina. Lithos 94, 46–65. http://dx.doi.org/10.1016/j.lithos.2006.06.011.
Pankhurst, R.J., Rapela, C.R., 1995. Production of Jurassic rhyolite by anatexis of the lower crust of Patagonia. Earth Planet. Sci. Lett. 134, 23–36. http://dx.doi.org/10.1016/0012-821X(95)00103-J.
Pankhurst, R.J., Leat, P.T., Sruoga, P., Rapela, C.W., Márquez, M., Storey, B.C., Riley, T. R., 1998. The Chon Aike province of Patagonia and related rocks in West Antarctica: a silicic large igneous province. J. Volcanol. Geotherm. Res. 81, 113–136. http://dx.doi.org/10.1016/S0377-0273(97)00070-X.
Pankhurst, R.J., Rapela, C.W., Loske, W.P., Márquez, M., Fanning, C.M., 2003. Chronological study of the pre-Permian basement rocks of southern Patagonia. J. South Am. Earth Sci. 16, 27–44. http://dx.doi.org/10.1016/S0895-9811(03)00017-8.
Pankhurst, R.J., Rapela, C.W., Fanning, C.M., Márquez, M., 2006. Gondwanide continental collision and the origin of Patagonia. Earth-Sci. Rev. 76, 235–257. http://dx.doi.org/10.1016/j.earscirev.2006.02.001.
Panza, J.L., 1994. Hoja Geológica 4969-II, Tres Cerros, Provincia de Santa Cruz, escala 1:250.000. Servicio Geológico Minero Argentino, Boletín 213.
Pearson, D.G., Irvine, G.J., Carlson, R.W., Kopylova, M.G., Ionov, D.A., 2002. The development of lithospheric keels beneath the earliest continents: time constraints using PGE and Re-Os isotope systematics. Geol. Soc. London, Spec. Publ. 199, 65–90. http://dx.doi.org/10.1144/GSL.SP.2002.199.01.04.
Pearson, D.G., Canil, D., Shirey, S.B., 2003. Mantle samples included in volcanic rocks: xenoliths and diamonds. In: Treatise on Geochemistry. Elsevier, pp. 171–275. http://dx.doi.org/10.1016/B0-08-043751-6/02005-3.
Pearson, D., Irvine, G., Ionov, D., Boyd, F., Dreibus, G., 2004. Re–Os isotope systematics and platinum group element fractionation during mantle melt extraction: a study of massif and xenolith peridotite suites. Chem. Geol. 208, 29–59. http://dx.doi.org/10.1016/j.chemgeo.2004.04.005.
Pérez-Gussinyé, M., Watts, A.B., 2005. The long-term strength of Europe and its implications for plate-forming processes. Nature 436, 381–384. http://dx.doi.org/10.1038/nature03854.
Peslier, A.H., Reisberg, L., Ludden, J., Francis, D., 2000. Os isotopic systematics in mantle xenoliths; age constraints on the Canadian Cordillera lithosphere. Chem. Geol. 166, 85–101. http://dx.doi.org/10.1016/S0009-2541(99)00187-4.
Pettersson, Å., Cornell, D.H., Moen, H.F.G., Reddy, S., Evans, D., 2007. Ion-probe dating of 1.2 Ga collision and crustal architecture in the Namaqua-Natal Province of southern Africa. Precambr. Res. 158, 79–92. http://dx.doi.org/10.1016/j.precamres.2007.04.006.
Poudjom Djomani, Y.H., O'Reilly, S.Y., Griffin, W.L., Morgan, P., 2001. The density structure of subcontinental lithosphere through time. Earth Planet. Sci. Lett. 184, 605–621. http://dx.doi.org/10.1016/S0012-821X(00)00362-9.
Pressi, L., 2008. Caracterização petrográfica e geoquímica de xenólitos mantélicos da região de Tres Lagos, Patagônia Argentina. Universidade Federal do Rio Grande do Sul.
Putirka, K.D., 2008. Thermometers and Barometers for Volcanic systems. Rev. Mineral. Geochem. 69, 61–120. http://dx.doi.org/10.2138/rmg.2008.69.3.
Ramos, V.A., 1984. Patagonia: ¿un continente paleozoico a la deriva? IX Congreso Geológico Argentino. San Carlos de Bariloche, 2, 311–325.
Ramos, V.A., 2002. Evolución Tectónica. In: Haller, M.J. (Ed.), Geología y Recursos Naturales de Santa Cruz, XV Congreso Geológico Argentino, I-23, pp. 365–387.
Ramos, V.A., 2008. Patagonia: a paleozoic continent adrift? J. South Am. Earth Sci. 26, 235–251. http://dx.doi.org/10.1016/j.jsames.2008.06.002.
Ramos, V.A., Kay, S.M., 1992. Southern Patagonian plateau basalts and deformation: Backarc testimony of ridge collisions. Tectonophysics 205, 261–282. http://dx.doi.org/10.1016/0040-1951(92)90430-E.
Ramos, V.A., Riccardi, A.C., Rolleri, E.O., 2004. Natural boundaries of Northern Patagonia. Rev. la Asoc. Geol. Argentina 59, 785–786.
Rapela, C.W., Pankhurst, R.J., Fanning, C.M., Grecco, L.E., 2003. Basement evolution of the Sierra de la Ventana Fold Belt: new evidence for Cambrian continental rifting along the southern margin of Gondwana. J. Geol. Soc. London 160, 613–628. http://dx.doi.org/10.1144/0016-764902-112.
Rapela, C.W., Pankhurst, R.J., Casquet, C., Fanning, C.M., Baldo, E.G., González-Casado, J.M., Galindo, C., Dahlquist, J., 2007. The Río de la Plata craton and the assembly of SW Gondwana. Earth-Sci. Rev. 83, 49–82. http://dx.doi.org/10.1016/j.earscirev.2007.03.004.
Reisberg, L., Lorand, J.-P., 1995. Longevity of sub-continental mantle lithosphere from osmium isotope systematics in orogenic peridotite massifs. Nature 376, 159–162. http://dx.doi.org/10.1038/376159a0.
Reisberg, L., Meisel, T., 2002. The Re-Os isotopic system: a review of analytical techniques. Geostand. Geoanal. Res. 26, 249–267. http://dx.doi.org/10.1111/j.1751-908X.2002.tb00633.x.
Rex, D.C., Tanner, P.W.G., 1982. Precambrian age for the gneisses at Cape Meredith in the Malvinas/Falkland islands. In: Craddock, Campbell (Ed.), Antarctic Geoscience, Symposium on Antarctic Geology and Geophysics. The University of Wisconsin Press, pp. 107–108.
Richards, P.C., Gatliff, R.W., Quinn, M.F., Fannin, N.G.T., Williamson, J.P., 1996. The geological evolution of the Falkland Islands continental shelf. In: Weddell Sea Tectonic and Gondwana Break-Up. Geological Society, London, Special Publications, pp. 105–128. http://dx.doi.org/10.1144/GSL.SP.1996.108.01.08.
Rieck, N., 2005. Evidências de heterogeneidade e metassomatismo no manto litosférico da região do Cerro de los Chenques, Patagônia – Argentina. Universidade Federal do Río Grande do Sul.
Ritsema, J., van Heijst, H.J., Woodhouse, J.H., 2004. Global transition zone tomography. J. Geophys. Res. Solid Earth 109. http://dx.doi.org/10.1029/2003JB002610.
Rivalenti, G., Mazzucchelli, M., Laurora, A., Ciuffi, S.I.A., Zanetti, A., Vannucci, R., Cingolani, C.A., 2004. The backarc mantle lithosphere in Patagonia, South America. J. South Am. Earth Sci. 17, 121–152. http://dx.doi.org/10.1016/j.jsames.2004.05.009.
Rivalenti, G., Mazzucchelli, M., Zanetti, A., Vannucci, R., Bollinger, C., Hémond, C., Bertotto, G.W., 2007. Xenoliths from Cerro de los Chenques (Patagonia): an example of slab-related metasomatism in the backarc lithospheric mantle. Lithos 99, 45–67. http://dx.doi.org/10.1016/j.lithos.2007.05.012.
Robb, L.J., Armstrong, R.A., Waters, D.J., 1999. The history of Granulite-Facies metamorphism and crustal growth from single zircon U-Pb geochronology: Namaqualand, South Africa. J. Petrol. 40, 1747–1770. http://dx.doi.org/10.1093/petroj/40.12.1747.
Rudnick, R.L., Walker, R.J., 2009. Interpreting ages from Re-Os isotopes in peridotites. Lithos 112, 1083–1095. http://dx.doi.org/10.1016/j.lithos.2009.04.042.
Sato, A.M., Tickyj, H., Llambías, E.J., Sato, K., 2000. The Las Matras tonalitic-trondhjemitic pluton, Central Argentina: Grenvillian-age constraints, geochemical characteristics, and regional implications. J. South Am. Earth Sci. 13, 587–610. http://dx.doi.org/10.1016/S0895-9811(00)00053-5.
Schalamuk, I., Zubia, M., Genini, A., Fernandez, R., 1997. Jurassic epithermal Au–Ag deposits of Patagonia, Argentina. Ore Geol. Rev. 12, 173–186. http://dx.doi.org/10.1016/S0169-1368(97)00008-5.
Schilling, M., Conceição, R.V., Mallmann, G., Koester, E., Kawashita, K., Hervé, F., Morata, D., Motoki, A., 2005. Spinel-facies mantle xenoliths from Cerro Redondo, Argentine Patagonia: petrographic, geochemical, and isotopic evidence of interaction between xenoliths and host basalt. Lithos 82, 485–502. http://dx.doi.org/10.1016/j.lithos.2004.09.028.
Schilling, M.E., Carlson, R.W., Conceição, R.V., Dantas, C., Bertotto, G.W., Koester, E., 2008. Re–Os isotope constraints on subcontinental lithospheric mantle evolution of southern South America. Earth Planet. Sci. Lett. 268, 89–101. http://dx.doi.org/10.1016/j.epsl.2008.01.005.
Schmitz, M.D., Bowring, S.A., 2001. The significance of U-Pb zircon dates in lower crustal xenoliths from the southwestern margin of the Kaapvaal craton, southern Africa. Chem. Geol. 172, 59–76. http://dx.doi.org/10.1016/S0009-2541(00)00236-9.
Schmitz, M.D., Bowring, S.A., 2004. Lower crustal granulite formation during Mesoproterozoic Namaqua-Natal collisional orogenesis, southern Africa. South Afr. J. Geol. 107, 261–284. http://dx.doi.org/10.2113/107.1-2.261.
Shirey, S.B., Walker, R.J., 1995. Carius tube digestion for low-blank rhenium-osmium analysis. Anal. Chem. 67, 2136–2141. http://dx.doi.org/10.1021/ac00109a036.
Shirey, S.B., Walker, R.J., 1998. The Re-Os isotope system in cosmochemistry and high-temperature geochemistry. Annu. Rev. Earth Planet. Sci. 26, 423–500. http://dx.doi.org/10.1146/annurev.earth.26.1.423.

Singer, B.S., Brown, L.L., Rabassa, J.O., Guillou, H., 2013. $^{40}Ar/^{39}Ar$ chronology of Late Pliocene and Early Pleistocene geomagnetic and glacial events in southern Argentina. In: Channell, J.E.T., Kent, D.V., Lowrie, W., Meert, J.G. (Eds.), Timescales of the Paleomagnetic Field. American Geophysical Union, Washington, D.C., pp. 175–190. http://dx.doi.org/10.1029/145GM13.

Smoliar, M.I., Walker, R.J., Morgan, J.W., 1996. Re-Os ages of Group IIA, IIIA, IVA, and IVB iron meteorites. Science 271, 1099–1102. http://dx.doi.org/10.1126/science.271.5252.1099.

Snow, J.E., Reisberg, L., 1995. Os isotopic systematics of the MORB mantle: results from altered abyssal peridotites. Earth Planet. Sci. Lett. 133, 411–421. http://dx.doi.org/10.1016/0012-821X(95)00099-X.

Stern, C.R., Frey, F.A., Futa, K., Zartman, R.E., Peng, Z., Kurtis Kyser, T., 1990. Trace-element and Sr, Nd, Pb, and O isotopic composition of Pliocene and Quaternary alkali basalts of the Patagonian Plateau lavas of southernmost South America. Contrib. Mineral. Petrol. 104, 294–308. http://dx.doi.org/10.1007/BF00321486.

Stern, C.R., Kilian, R., Olker, B., Hauri, E.H., Kyser, T.K., 1999. Evidence from mantle xenoliths for relatively thin (#100 km) continental lithosphere below the Phanerozoic crust of southernmost South America. Lithos 48, 217–235. http://dx.doi.org/10.1016/S0024-4937(99)00030-4.

Stone, P., Kimbell, G.S., Richards, P.C., 2009. Rotation of the Falklands microplate reassessed after recognition of discrete Jurassic and Cretaceous dyke swarms. Pet. Geosci. 15, 279–287. http://dx.doi.org/10.1144/1354-079309-847.

Storey, B.C., Curtis, M.L., Ferris, J.K., Hunter, M.A., Livermore, R.A., 1999. Reconstruction and break-out model for the Falkland Islands within Gondwana. J. Afr. Earth Sci. 29, 153–163. http://dx.doi.org/10.1016/S0899-5362(99)00086-X.

Tassara, A., Swain, C., Hackney, R., Kirby, J., 2007. Elastic thickness structure of South America estimated using wavelets and satellite-derived gravity data. Earth Planet. Sci. Lett. 253, 17–36. http://dx.doi.org/10.1016/j.epsl.2006.10.008.

Thomas, R.J., Agenbacht, A.L.D., Cornell, D.H., Moore, J.M., 1994. The Kibaran of southern Africa: tectonic evolution and metallogeny. Ore Geol. Rev. 9, 131–160. http://dx.doi.org/10.1016/0169-1368(94)90025-6.

Thomas, R.J., Jacobs, J., Eglington, B.M., 2000. Geochemistry and isotopic evolution of the Mesoproterozoic Cape Meredith Complex, West Falkland. Geol. Mag. 137, 537–553. http://dx.doi.org/10.1017/S0016756800004519.

Torsvik, T.H., Cocks, L.R.M., 2013. Gondwana from top to base in space and time. Gondwana Res. 24, 999–1030. http://dx.doi.org/10.1016/j.gr.2013.06.012.

Vujovich, G.I., Fernandes, L.A.D., Ramos, V.A., 2004. Cuyania: an exotic block to Gondwana — introduction. Gondwana Res. 7, 1005–1007. http://dx.doi.org/10.1016/S1342-937X(05)71080-7.

Walker, R., Carlson, R., Shirey, S., Boyd, F.R., 1989. Os, Sr, Nd, and Pb isotope systematics of southern African peridotite xenoliths: implications for the chemical evolution of subcontinental mantle. Geochim. Cosmochim. Acta 53, 1583–1595. http://dx.doi.org/10.1016/0016-7037(89)90240-8.

Wang, J., 2007. Oxidation and metasomatism of lithospheric mantle beneath the southern South America. University of Ottawa.

Wang, J., Hattori, K.H., Kilian, R., Stern, C.R., 2007. Metasomatism of sub-arc mantle peridotites below southernmost South America: reduction of fO_2 by slab-melt. Contrib. Mineral. Petrol. 153, 607–624. http://dx.doi.org/10.1007/s00410-006-0166-4.

Wang, J., Hattori, K.H., Li, J., Stern, C.R., 2008. Oxidation state of Paleozoic subcontinental lithospheric mantle below the Pali Aike volcanic field in southernmost Patagonia. Lithos 105, 98–110. http://dx.doi.org/10.1016/j.lithos.2008.02.009.

Wareham, C.D., Pankhurst, R.J., Thomas, R.J., Storey, B.C., Grantham, G.H., Jacobs, J., Eglington, B.M., 1998. Pb, Nd, and Sr isotope mapping of Grenville-age crustal provinces in Rodinia. J. Geol. 106, 647–660. http://dx.doi.org/10.1086/516051.

Watts, A.B., 2001. Isostasy and Flexure of the Lithosphere. Cambridge University Press.

Will, T.M., Zeh, A., Gerdes, A., Frimmel, H.E., Millar, I.L., Schmädicke, E., 2009. Palaeoproterozoic to Palaeozoic magmatic and metamorphic events in the Shackleton Range, East Antarctica: constraints from zircon and monazite dating, and implications for the amalgamation of Gondwana. Precambr. Res. 172, 25–45. http://dx.doi.org/10.1016/j.precamres.2009.03.008.